

# AIRCRAFT MEASUREMENTS OF THE IMPACTS OF POLLUTION AEROSOLS ON CLOUDS AND PRECIPITATION OVER THE SIERRA NEVADA

*Prepared For:*  
**California Energy Commission**  
Public Interest Energy Research Program

*Prepared By:*  
Woodley Weather Consultants  
Institute of Earth Sciences, The Hebrew  
University of Jerusalem  
Seeding Operation & Atmospheric  
Research  
Desert Research Institute, University of  
Nevada



Arnold Schwarzenegger  
*Governor*

PIER PROJECT REPORT

March 2008  
CEC-500-2008-015



California Climate Change Center  
Report Series Number 2008-001



**Prepared By:**

William L. Woodley  
Woodley Weather Consultants, 11 White Fir Court, Littleton CO 80127

Daniel Rosenfeld  
Eyal Freud  
Institute of Earth Sciences, The Hebrew University of Jerusalem,  
Israel

Duncan Axisa  
Seeding Operations & Atmospheric Research, POB 130, Plains TX  
79355

James G. Hudson  
Desert Research Institute, University of Nevada, Reno, Nevada

Commission Contract No. 500-02-004, UC MR-042

**Prepared For:**

Public Interest Energy Research (PIER) Program

**California Energy Commission**

Guido Franco

**Contract Manager**

Kelly Birkinshaw

**Program Area Lead**

**Energy-Related Environmental Research**

Ken Koyama

**Acting Office Manager**

**Energy Systems Research**

Martha Krebs

**Deputy Director**

**ENERGY RESEARCH & DEVELOPMENT DIVISION**

Melissa Jones

**Executive Director**

**DISCLAIMER**

This report was prepared as the result of work sponsored by the California Energy Commission. It does not necessarily represent the views of the Energy Commission, its employees or the State of California. The Energy Commission, the State of California, its employees, contractors and subcontractors make no warrant, express or implied, and assume no legal liability for the information in this report; nor does any party represent that the uses of this information will not infringe upon privately owned rights. This report has not been approved or disapproved by the California Energy Commission nor has the California Energy Commission passed upon the accuracy or adequacy of the information in this report.



## Acknowledgments

The authors gratefully acknowledge the major contributions that the pilots made to the success of the Suppression of Precipitation (SUPRECIP) field effort. Dr. David Prentice piloted the Cheyenne II cloud physics aircraft during SUPRECIP-1, and Mr. Gary Walker, Manager of the Seeding Operations and Atmospheric Research (SOAR) program of the Sandyland Underground Water Conservation District, piloted this aircraft in SUPRECIP-2. Mr. Kevin McLaughlin piloted the Cessna 340 aerosol aircraft. The authors also acknowledge Dr. Don Collins and Ms. Crystal Reed of Texas A&M University for their support with the differential mobility analyzer/Tandem Differential Mobility Analyzer (DMA/TDMA) system and Ing. Grazio Axisa for maintaining the aircraft instruments in SUPRECIP-2.

The research was supported by the Public Interest Energy Research (PIER) Program of the California Energy Commission. The authors especially appreciate the enthusiastic encouragement of Mr. Guido Franco of PIER throughout the research effort.

Please cite this report as follows:

Woodley, William L., Daniel Rosenfeld, Duncan Axisa, Eyal Freud, and James G. Hudson. 2008. *Aircraft Measurements of the Impacts of Pollution Aerosols on Clouds and Precipitation Over the Sierra Nevada*. California Energy Commission, PIER Energy-Related Environmental Research. CEC-500-2008-015.



## Preface

The Public Interest Energy Research (PIER) Program supports public interest energy research and development that will help improve the quality of life in California by bringing environmentally safe, affordable, and reliable energy services and products to the marketplace.

The PIER Program, managed by the California Energy Commission (Energy Commission), conducts public interest research, development, and demonstration (RD&D) projects to benefit California's electricity and natural gas ratepayers. The PIER Program strives to conduct the most promising public interest energy research by partnering with RD&D entities, including individuals, businesses, utilities, and public or private research institutions.

PIER funding efforts are focused on the following RD&D program areas:

- Buildings End-Use Energy Efficiency
- Energy-Related Environmental Research
- Energy Systems Integration
- Environmentally Preferred Advanced Generation
- Industrial/Agricultural/Water End-Use Energy Efficiency
- Renewable Energy Technologies
- Transportation

In 2003, the California Energy Commission's Public Interest Energy Research (PIER) Program established the **California Climate Change Center** to document climate change research relevant to the states. This center is a virtual organization with core research activities at Scripps Institution of Oceanography and the University of California, Berkeley, complemented by efforts at other research institutions. Priority research areas defined in PIER's five-year Climate Change Research Plan are: monitoring, analysis, and modeling of climate; analysis of options to reduce greenhouse gas emissions; assessment of physical impacts and of adaptation strategies; and analysis of the economic consequences of both climate change impacts and the efforts designed to reduce emissions.

**The California Climate Change Center Report Series** details ongoing center-sponsored research. As interim project results, the information contained in these reports may change; authors should be contacted for the most recent project results. By providing ready access to this timely research, the center seeks to inform the public and expand dissemination of climate change information, thereby leveraging collaborative efforts and increasing the benefits of this research to California's citizens, environment, and economy.

*Aircraft Measurements of the Impacts of Pollution Aerosols on Clouds and Precipitation Over the Sierra Nevada* is the final report for the Suppression of Precipitation (SUPRECIP-2) project (500-02-004, MR-042) conducted by Woodley Weather Consultants.

For more information on the PIER Program, please visit the Energy Commission's website [www.energy.ca.gov/pier/](http://www.energy.ca.gov/pier/) or contact the Energy Commission at (916) 654-5164.





# Table of Contents

Preface.....	iii
Abstract .....	xi
Executive Summary .....	1
Technical Summary .....	3
1.0 Introduction.....	9
2.0 The SUPRECIP Program .....	11
2.1 The SUPRECIP-1 Effort .....	14
2.2 The SUPRECIP-2 Effort .....	18
3.0 Results of SUPRECIP-2 Analyses.....	19
3.1 Establishing a Direct Link Between the Sub-Cloud Aerosols and Cloud Microphysical Structure .....	19
3.1.1 A Case Study: February 28, 2006 .....	19
3.1.2 Ensemble Results .....	29
3.2 Diurnal Aerosol Variability .....	32
3.3 Spatial Aerosol Distribution .....	40
4.0 Discussion.....	47
5.0 Conclusions .....	49
6.0 References.....	51
7.0 Glossary .....	53

## List of Figures

Figure 1. The SOAR Cheyenne II cloud physics aircraft .....	12
Figure 2. Scatter plot of the median effective radii ( $r_e$ ) determined by aircraft (Aircraft $r_e$ ) for individual cloud passes vs. the median $r_e$ inferred from the multi-spectral satellite imagery (Satellite median $r_e$ ) for the altitudes and temperatures of the aircraft cloud passes for clouds in regions where the cloud passes were made. The comparisons were made for data obtained on February 7 and March 4, 2005. ....	15
Figure 3. Cloud drop number concentrations as a function of the CCN concentration before and after cloud pass at a supersaturation of 0.5%. Each point represents the median (blue) and maximum (red) droplet concentrations for one cloud pass. The best-fit equations are as shown.....	16
Figure 4. The effective diameter ( $D_{eff}$ ) of the cloud drops normalized to the cloud liquid water content (LWC) by the expression $D_{eff} / LWC^{0.333}$ , as a function of the CCN concentrations for each cloud pass.....	17
Figure 5. The Oakland rawinsonde of March 1, 2006, at 00Z, which is near the time that the aircraft flew near Oakland .....	19
Figure 6. The tracks of the Cloud (black) and Aerosol (colored) airplanes. The time marks every 5 minutes are posted on the aerosol aircraft tracks and labeled every 10 minutes. The CCN concentrations adjusted to supersaturation of 0.9% are shown in the color scale. The relative height of the aerosol aircraft above sea level is shown by the vertical displacement of the track. The clouds measured by the cloud physics aircraft are marked with green circles and numbered sequentially. ....	20
Figure 7. Plot of cloud droplet diameters as a function of liquid water content (LWC) for Cloud 1 over the western slopes of the Sierra Nevada (see location in Figure 6). The modal liquid water drop diameter occurs at the droplet size having the greatest water content. Cloud 1 developed in an air mass that had 300–800 CCN $cm^{-3}$ . Panel A shows the Cloud Droplet Probe (CDP)-measured LWC distribution. Each line represents the gross cloud drop size distribution of a whole cloud pass. The legend of the lines is composed of the pass height [m] to the left of the decimal point, and the pass starting GMT time [hhmmss] to the right of the point. The passes are ordered in altitude ascending order. Note the increase in cloud drop volume modal size with increasing cloud depth. Panel B shows the combined distributions of the CDP and the cloud imaging probe (CIP). According to the figure the large precipitation particles were well separated from the cloud drop size distribution, indicating lack of appreciable coalescence. ....	22
Figure 8. Same as Figure 7, but for Cloud 2 over the hills 60 km NE of Monterey (see location in Figure 6). It developed in an air mass that had 100 CCN $cm^{-3}$ . The cloud drops are quite large and the distribution continues smoothly into the rain drop sizes. This indicates active warm rain processes. ....	23

- Figure 9. Same as Figure 7, but for Cloud 3 over the hills near Big Sur (see location in Figure 6). It developed in an air mass that had about 40 CCN cm<sup>-3</sup>. The cloud drops are very large, and the distribution continues smoothly into the rain drop sizes. This indicates very active warm rain processes. .... 24
- Figure 10. Same as Figure 7, but for single heights in clouds 4–8 in a cross-section from the Pacific Ocean to Sacramento, marked by clouds 4, 5, 6, 7, and 8, respectively. The respective approximated CCN concentrations from the measurements made by the aerosol aircraft are denoted by the circles and are located under the peaks of the DL plots having the same color. The CCN values are to be read from the right ordinate. The CCN concentrations are: Cloud 4: 70; Cloud 5: 100; Cloud 6: 300; Cloud 7: 600; Cloud 8: 800 cm<sup>-3</sup>. The drops become markedly smaller with increasing CCN concentrations. Warm rain ceases at Cloud 3, where 300 CCN cm<sup>-3</sup> were present. .... 25
- Figure 11. Same as Figure 7 but for the vertical cross-section in Cloud 8 over Sacramento (see location in Figure 6). It developed in an air mass that had about 800 CCN cm<sup>-3</sup>. The cloud drops are very small and do not expand much with height into raindrops, again as in Cloud 1. .... 26
- Figure 12. An image from the MODIS on NASA’s Aqua satellite of the clouds in Central California on February 28, 2006, at 21:00Z. The color scale is a composite following Rosenfeld and Lensky (1998) where the red is modulated by the visible solar reflectance, blue modulated by the thermal temperature, and green modulated by the 3.7 μm solar reflectance component. The green is brighter for smaller cloud particles. Therefore, the polluted clouds with small drops appear yellow (see Areas 1, 5 and 6); whereas the ice clouds appear red (see areas 3 and 7). Pristine water clouds appear magenta (see Area 8), because they have low green (large water drops) and high blue (warm temperature). The line graphs provide the relations between the satellite-indicated cloud top temperatures and the cloud top particle effective radii. At the foothills in Areas 1 and 5 the cloud top effective radius is much smaller than the precipitation threshold of 14 μm (Rosenfeld and Gutman 1994), whereas the effective radius of 18 μm in Area 8 is much larger than the precipitation threshold. .... 28
- Figure 13. Scatter plot of the modal liquid water drop diameter (DL) vs. the distance above cloud-base height. Each plotted point has been colorized according to the scale on the right where browns, reds, and yellows indicate cloud passes with high sub-cloud CCN concentrations and blue points indicate cloud passes having low sub-cloud CCN concentrations. The vertical line marks the threshold for formation of precipitation-sized drops, when DL = 24 μm. The two lines are the approximated contours of 225 and 1000 CCN cm<sup>-3</sup>, as done by the contouring routine of MATLAB. The contouring was done after transferring the individual data points to a surface by linear interpolation and initial smoothing. .... 30
- Figure 14. The global context of the dependence of the drop size modal LWC DL on height above cloud base and temperature. The lines, according to their order in the legend, are:

Amazon pyro-Cb, smoky, transition, pristine over land and pristine over ocean clouds (Andreae et al. 2004); Thailand pre-monsoon smoky and monsoon relatively clean clouds (Andreae et al. 2004); Argentina microphysically continental hail storms (Rosenfeld et al. 2006); California polluted and pristine clouds (Figure 13 of this study). The vertical line at DL=24 $\mu\text{m}$ represents the warm rain threshold. ....	31
Figure 15. The flight tracks for the aerosol (red) and cloud physics (black) aircraft for the three flights on March 2, 2006 .....	33
Figure 16. Plots as a function of height (in m) of the CN (total) and CCN concentrations ( $\text{cm}^{-3}$ ) measured by the aerosol aircraft on the three March 2, 2006, flights during its step-climb to 3 km altitude (top three panels) and the corresponding plots as a function of height (in m) of the droplet concentrations and sizes (effective radius) measured by the cloud physics aircraft on its three flights of the day (lower three panels). The red dots in the upper panels show the adjusted CCN measurements (to 0.9% supersaturation) only during horizontal flight (ascent rate $< \pm 3$ m/s). This adjustment was done to take into account the varying super-saturations (in the range of $\sim 0.1\%$ – $0.85\%$ ) and because decreases in the raw CCN concentrations were noted while the aircraft was ascending. The black dots are the raw CCN measurements.....	34
Figure 17. Plots of the CCN (at two supersaturations) and CN aerosols observed at the Blodgett Forest Research Station (1314 m elevation) on March 2, 2006. Despite a gap in the data stream, a strong diurnal cycle is evident in the plots. The vertical blue lines enclose the period (0901 to 1621 PST) when the research aircraft were flying on this day. ....	35
Figure 18. Mean time (Pacific Standard Time) plots for February (black) and for March (red) 2006 of the CCN (top) and CN total aerosol (middle) concentrations measured at the Blodgett Research Station by Dr. Jim Hudson of the Desert Research Institute. Plots of the ratio CCN/CN in February (black) and March (red) are given in the bottom panel. The CCN aerosol measurements were made at a supersaturation of 1%. ....	37
Figure 19. Scatter plot of the orographic precipitation enhancement factor ( $R_o$ ) in the fall (blue points) and spring (red points) for the years 1885 to 2000 for Cuyamaca vs. San Diego (panel A), where $R_o$ is defined as the ratio of the precipitation at the mountain station (Cuyamaca) to the precipitation at the upwind lowland plains or coastal station. Panel B shows the same for $R_o$ between a gauge cluster in Placerville versus a cluster in the Sacramento area. The apparent effect of pollution on precipitation at the mountain station is obtained by taking the ratio of $R_o$ at the end of the period of interest to $R_o$ at the outset of the period, where the ending and starting $R_o$ values are obtained from the best-fit line to the scatter plot. In these instances the analyses were done separately for the fall and spring months. Although precipitation losses occurred in both the fall and spring, the losses were greater in the spring (i.e., -27% to -30%) than in the fall months (i.e., -17% to -20%) because the sun is stronger in the spring months during which convective currents would more readily transport pollution aerosols to higher altitudes.....	39

Figure 20. A colorized plot summary of the CCN measurements made on all flight days without wind partitioning during SUPRECIP-2 when the aerosol aircraft was flying below 5000 ft, almost exclusively below cloud base. The X and Y axes are deg. longitude and deg. latitude, respectively. According to the legend, the portions of the track when the CCN readings exceeded 1000/cm<sup>3</sup> are orange changing to dark brown at readings of 4000/cm<sup>3</sup>. The portions of the track when the CCN readings were < 100/cm<sup>3</sup> begin at light blue and change to dark blue for the lowest CCN concentrations. Note that the highest CCN readings were in the Sacramento area and southeastward to the Sierra foothills..... 41

Figure 21. Surface streamline map for Central and Northern California at 00 UTC on March 1, 2006, produced by NOAA's Air Resources Laboratory. The flight tracks of the cloud physics (black) and aerosol aircraft (blue with red dots every 5 minutes along the track) have been superimposed on the streamline presentation. The flight tracks are the same as those presented in Figure 6..... 42

Figure 22. The same as for Figure 20 but for southwesterly surface wind flows. Units for the X and Y axes are degrees west longitude and degrees north latitude, respectively. .... 43

Figure 23. The same as in Figure 20 but for the CN (total aerosol) measurements ..... 44

Figure 24. The same as for Figure 20 but for the ratio of CCN to CN. The colorized portion of the track can be related to CCN/CN from the figure legend. .... 45

## List of Tables

Table 1. Data sets from the aerosol aircraft ..... 12

Table 2. Data sets from the cloud physics aircraft..... 13



## Abstract

Recent publications suggest that anthropogenic aerosols suppress orographic precipitation in California and elsewhere. A field campaign (SUPRECIP: Suppression of Precipitation) was conducted to investigate this hypothesized aerosol effect. The campaign consisted of aircraft measurements of the polluting aerosols, the composition of the clouds ingesting them, and the way the precipitation-forming processes are affected. SUPRECIP was conducted during February and March of 2005 and February and March of 2006. The flights documented aerosols and orographic clouds flowing into the central Sierra Nevada from upwind densely populated industrialized/urbanized areas and contrasted them with the aerosols and clouds downwind of the sparsely populated areas in the northern Sierra Nevada.

SUPRECIP found that the aerosols transported from the coastal regions are augmented by local sources in the Central Valley, resulting in high concentrations of aerosols in the eastern parts of the Central Valley and the Sierra foothills. This pattern is consistent with the detected patterns of suppressed orographic precipitation that occur primarily in the southern and central Sierra Nevada but not in the north. The precipitation suppression occurs mainly in the orographic clouds that are triggered from the boundary layer over the foothills and propagate over the mountains, although the elevated orographic clouds that form at the crest are minimally affected. The clouds are affected mainly during the second half of the day and the subsequent evening, when solar heating mixes the boundary layer up to cloud bases. Local, yet unidentified non-urban sources are suspected to play a major role.

**Keywords:** Aerosols, pollution aerosols, orographic precipitation, clouds, Sierra Nevada Mountains, Sierra Nevada winter snowfall, suppression of precipitation due to pollution, atmospheric measurements from aircraft





# Executive Summary

## Introduction

Woodley Weather Consultants conducted highly focused research for the Public Interest Energy Research (PIER) Program of the California Energy Commission to document and model the effects of urban and industrial air pollution in California on clouds, precipitation, and stream flows in mountainous terrain downwind of the pollution sources. Orographic precipitation (that is, precipitation over the mountains) has decreased over California's Sierra Nevada mountains, and satellite data and other evidence suggest that pollution aerosols transported from urban areas west of the Sierra Nevada contribute to this decreased precipitation.

## Project Purpose

This project sought to document the "ingestion" of pollution aerosols (that is, their incorporation into the orographic clouds) as the clouds were formed and moved uphill. It also sought to document the number, sizes, and concentrations of the aerosols and the resulting internal cloud microphysical structure. This information was used to analyze the orographic precipitation process to better determine the role of those pollution aerosols in suppressing precipitation.

## Project Objectives

The research objectives were to measure atmospheric aerosols in pristine and polluted clouds, to document the effect of aerosols on orographic cloud formation. Specific objectives included the following:

- Systematically measure the pollution aerosols at low to mid levels in urban and downwind areas using research aircraft.
- Demonstrate a connection between the documented cloud structures and the ingested aerosols.
- Validate the multispectral satellite inferences of cloud structure and the effect of pollutants on cloud processes—especially precipitation suppression.

The Suppression of Precipitation (SUPRECIP) Experiment was conducted in two phases, using research aircrafts and satellite information. Phase 1 (SUPRECIP 1) was conducted during February and March 2005, and Phase 2 (SUPRECIP 2) was conducted in February and March 2006. SUPRECIP 2 focused on the orographic storm events in the Sierra Nevada that were lacking in 2005. Both phases employed a Cheyenne II turbo-prop cloud physics research aircraft, however, SUPRECIP 2 added an additional Cessna 340 aerosol aircraft to collect a more comprehensive data set.

## **Project Outcomes**

Research results showed the following:

- The regions of precipitation loss in California have higher concentrations of cloud condensation nuclei (aerosols that act as seeds for the formation of water droplets) than more pristine areas.
- There is a direct link between the cloud condensation nuclei aerosols and the altered cloud structures, resulting in suppressed droplet growth and precipitation.
- As the number of condensation nuclei in a cloud rises, cloud depth must increase for the cloud to develop precipitation. Thus, clouds that ingest pollution aerosols require greater cloud depths and more formation time for the drops to reach precipitation size. This phenomenon results in less precipitation in orographic clouds, given their relatively short life span.
- Local generation of pollution aerosols in the Central Valley appears to be a greater problem for orographic precipitation than the transport of pollution from the urbanized, industrialized coastal regions or inland from the Pacific.

## **Conclusions**

The SUPRECIP experiment documented agreement between physical measurements and satellite data, both of which indicate that pollution aerosols result in reduced Sierra precipitation. Thus, it appears that pollution is affecting Sierra orographic clouds and precipitation (and, therefore, stream flows) detrimentally.

Because the important role of pollution aerosols in the Central Valley, future research should document the sources and chemical constituency of Central Valley aerosols. Not all of the aerosols act as cloud seeds (cloud condensation nuclei), so future research should be funded to investigate the sources of particles that affect cloud formation.

## **Benefits to California**

This research has established a link between the pollution aerosols produced in the state's urban areas and Central Valley and their suppressive effect on the microstructure of Sierra orographic clouds and their resultant precipitation. Related research has shown that California has been losing precipitation (and stream flows from that precipitation) across the Sierra Nevada range over the past 50 years. These losses have not yet affected California's water supply noticeably because they have been masked in many places by an increasing trend of natural precipitation over the state. This study's results provide state officials with a more complete demonstration of these aerosols' negative effect on California's water availability and the need for additional studies to reduce this effect.

# Technical Summary

## Introduction

Woodley Weather Consultants is conducting highly focused research for the Public Interest Energy Research (PIER) Program of the California Energy Commission to document and model the effects of urban and industrial air pollution in California on clouds, precipitation, and stream flows in mountainous terrain downwind of the pollution sources. Orographic precipitation (that is, precipitation over the mountains) has decreased over California's Sierra Nevada mountains, and satellite data and other evidence suggest that pollution aerosols transported from urban areas west of the Sierra Nevada contribute to this decreased precipitation.

## Project Purpose

This project sought to document the ingestion of the pollution aerosols by the orographic clouds as they formed and moved uphill, as well as the number, sizes, and concentrations of the aerosols and the resulting internal cloud microphysical structure. This information would then be used to analyze the orographic precipitation process and better determine the role of those pollution aerosols in suppressing precipitation.

## Project Objectives

The research objectives were to measure atmospheric aerosols in pristine and polluted clouds and to document the aerosols' impact on cloud-base microstructure, on the evolution with height of the cloud drop-size distribution, and on the development of precipitation under warm and mixed-phase processes. Specific objectives included the following:

- Systematically "map" the pollution aerosols at low to mid levels in urban and downwind areas using research aircraft.
- Demonstrate a connection between the documented cloud structures and the ingested aerosols.
- Validate the multi-spectral satellite inferences of cloud structure and the effect of pollutants on cloud processes—especially precipitation suppression.

The Suppression of Precipitation (SUPRECIP) Experiment was conducted to document the effect of the aerosols on cloud properties. It was conducted in two phases, using research aircraft. Phase 1 (SUPRECIP 1) was conducted during February and March 2005, and Phase 2 (SUPRECIP 2) was conducted in February and March 2006, to better document aerosols in the atmospheric boundary layer and to measure a better set of orographic cloud conditions than those found in the SUPRECIP 1 time frame. SUPRECIP 2 focused on the orographic storm events in the Sierra Nevada that were lacking in 2005. Both phases employed a Cheyenne II turbo-prop cloud physics research aircraft, and SUPRECIP 2 added an additional Cessna 340

aerosol aircraft, to collect a more comprehensive data set. The SUPRECIP 1 analyses focused on case studies and subsets of the overall data set. The SUPRECIP 2 analyses focused on the entire set of data taken by the two cloud physics aircraft.

## **Project Outcomes**

The project's initial, pre-flight research had indicated the following:

- Urban and industrialized regions of the world produce pollution aerosols that are mostly in submicron sizes because the efforts to remove pollutants have been most effective for larger particle sizes.
- The smallest aerosols, acting as "cloud condensation nuclei," are the most suppressive of precipitation-forming processes in clouds.
- Cloud condensation nuclei pollution aerosols can act to invigorate long-living convective clouds or suppress precipitation formation in shallow orographic clouds that have short-living cloud elements.
- The winter orographic precipitation enhancement factor, called *Ro*, has been decreasing at many locations in the world, including California, most of the western United States, Australia, South Africa, Portugal, Israel, France, Switzerland, Morocco, China, Canada, Greece, and Spain.
- Although both absolute precipitation amounts and the precipitation enhancement factor are affected by fluctuations in the atmospheric circulation patterns, these climatic fluctuations cannot explain the observed trends in the orographic precipitation enhancement factor.
- Although the trends of aerosols are available in the United States only since 1988, aerosol measurements from the Interagency Monitoring of Protected Visual Environments aerosol monitoring network show that the negative trends in the orographic precipitation enhancement factor are associated with elevated concentrations of fine aerosols (particulate matter less than 2.5 micrometers in diameter).
- The research that Woodley Weather Consultants has conducted for PIER has shown that the regions of precipitation loss in California have higher concentrations of cloud condensation nuclei pollution aerosols than more pristine areas and that there is a direct link between the cloud condensation nuclei aerosols and the altered cloud structures, including suppressed droplet growth and precipitation.
- Recent research involving Mount Hua in China has shown a direct link between reduced visibilities on the mountain, which are a manifestation of the presence of pollution aerosols, and the loss of precipitation there as manifested by long-term decreases in the orographic precipitation enhancement factor.
- The regions of decreased orographic precipitation enhancement factor in California and Israel have been shown to be regions of decreased stream flows and decreased spring outflows, respectively. Thus, the regions of decreased precipitation enhancement factor are regions experiencing real losses in surface water.

- Glaciogenic cloud seeding for precipitation enhancement has worked to offset the losses due to pollution in Israel. Consequently, long-term cloud seeding over the Sierra in California may have acted over the years to compensate for the precipitation losses in the polluted portions of the Sierra.

The flights of SUPRECIP 1 documented the aerosols and orographic clouds in the central Sierra Nevada and contrasted them with the aerosols and clouds downwind of the sparsely populated areas in the northern Sierra Nevada. The main results from SUPRECIP 1 are:

- The in situ aircraft measurements of the cloud microstructure validated the satellite retrievals of cloud particle effective radius and microphysical phase.
- Ample supercooled drizzle drops were found in the pristine orographic clouds with only few tens of drops per cubic centimeter, and no drizzle with small concentrations of graupel were found in clouds with drop number concentrations of approximately 150 per cubic centimeter .
- The pristine clouds occurred in air masses that were apparently decoupled from the boundary layer in the early morning, whereas the more microphysically continental clouds occurred during the afternoon after the surface inversion over the Central Valley disappeared.

The use of the research aircraft made possible the documentation of differences in cloud microstructure associated with differences in cloud condensation nuclei that were related visibly to air pollution. The aircraft measurements validated the satellite data that was previously used to link the pollution aerosols with suppressed precipitation. Both the aircraft and satellite measurements documented that aerosols have a direct effect on in-cloud structure, suggesting a connection between pollution aerosols and altered cloud processes. This effect may help to explain the long-term losses in Sierra orographic precipitation.

Data from SUPRECIP 1 were a major step in showing a connection between the cloud condensation nuclei aerosols and the cloud microphysical properties; however, it did not prove that sub-micron pollution aerosols are systematically compromising California's water supply. The SUPRECIP 2 was necessary to show the connection between the aerosols and the precipitation from the polluted clouds.

The addition of the aerosol aircraft during SUPRECIP 2 made it possible to measure the cloud condensation nuclei below the bases of clouds being studied above by the Cheyenne II cloud physics aircraft. This enabled researchers to show that the higher the cloud condensation nuclei counts, the greater the cloud depth needed for the cloud to develop precipitation. Thus, clouds that ingest pollution aerosols require greater cloud depths for the drops to reach precipitation size.

## **Conclusions**

The SUPRECIP experiment documented agreement between physical measurements and satellite data, both of which indicate that pollution aerosols result in reduced Sierra precipitation. Thus, it appears that pollution is affecting Sierra orographic clouds and precipitation (and therefore, stream flows) detrimentally.

The key uncertainty at the outset of SUPRECIP was whether the altered cloud properties were attributable to the ingestion of pollution aerosols. SUPRECIP 2 demonstrated the direct linkage between these aerosols and the regions in the central and southern Sierra Nevada that have suffered losses of orographic precipitation and stream flows. The analysis of several hundred cloud passes shows that in regions where high concentrations of cloud condensation nuclei were measured by the base aerosol aircraft, the clouds had to grow to greater depths to develop precipitation than did the clouds growing in regions of small cloud condensation nuclei concentrations.

SUPRECIP's spatial and temporal documentation of the aerosols also raised a new issue. Although the initial source of the pollution aerosols was clearly the urbanized coastal region, the pollution aerosols in the Central Valley to the Sierra foothills cannot be explained by simple transport of the pollutants from the coastal urban areas. There is clearly a major source of pollution aerosols in the Central Valley itself and these aerosols are concentrated primarily over the Central Valley from just to the north of Sacramento southward along the foothills to south of Fresno. This is the same region that has been shown through statistical analysis of precipitation and stream flow records to suffer the greatest loss of winter precipitation and subsequent stream flows.

The study also demonstrated that the pollution aerosols show a strong diurnal oscillation. In the morning these aerosols are concentrated at low levels, but by late afternoon they have been transported upward because of the afternoon heating. Thus, the regional clouds are most affected by the pollutants late in the day.

The evidence amassed from SUPRECIP and the ancillary precursor effort conducted by the authors indicates that the precipitation and stream flow losses are real and due primarily to the ingestion of pollutants by orographic clouds over the Sierra Nevada. Further, the results of model simulations demonstrating the detrimental effects of pollutants on Sierra orographic precipitation give additional weight to the hypothesis put forth at the outset of this research effort that anthropogenic aerosols are responsible for the decrease in the orographic precipitation enhancement factor in the California Sierra.

## **Recommendations**

Because the local generation of the pollution aerosols in the Central Valley appears to be a greater problem than the transport of pollution of from the urbanized, industrialized coastal regions or inland from the Pacific, future research should document the sources and chemical constituency of the aerosols in the Central Valley.

In addition, research should be conducted to investigate whether glaciogenic cloud seeding for precipitation enhancement over the Sierra Nevada mountains has worked to offset the precipitation losses due to pollution.

### **Benefits to California**

This research has established a link between the pollution aerosols produced in the state's urban areas and Central Valley and their suppressive effect on the microstructure of Sierra orographic clouds and their resultant precipitation. Ancillary research has shown that California has been losing precipitation over (and stream flows from) the Sierra Nevada Range over the past 50 years. These losses have not yet affected California's water supply noticeably because they have been masked in many places by an increasing trend of natural precipitation over the state and possibly due to the effects of cloud seeding. This study's results provide state officials with information they need to plan and implement remedial action to mitigate the detrimental effect of pollution on California's water supply.





## 1.0 Introduction

Anthropogenic aerosols from major coastal urban areas pollute the pristine maritime air masses that flow inland from the ocean and bring much of the precipitation, especially over the mountain ranges. Satellite observations indicate that urban aerosols reduce cloud drop effective radii ( $r_e$ ) and suppress both warm and mixed-phase precipitation in the clouds downwind of the urban areas (Rosenfeld 2000). This prompted studies that quantified the precipitation losses over topographical barriers downwind of major coastal urban areas in the western United States (particularly in California) and in Israel. These results showed losses of 15%–25% of the annual precipitation over the western slopes of the hills (Givati and Rosenfeld 2004, 2005; Rosenfeld and Givati 2006; Givati and Rosenfeld 2007). The suppression occurs mainly in the relatively shallow orographic clouds within the cold air mass of cyclones. The suppression that occurs over the upslope side is coupled with similar percentage enhancement on the much drier downslope side of the hills.

These results are consistent with other studies that have shown that higher cloud condensation nuclei (CCN) concentrations increase cloud droplet concentrations, decrease cloud droplet sizes, and reduce droplet coalescence and thus, precipitation (e.g., Hudson and Yum 2001; McFarquhar and Heymsfield 2001; Yum and Hudson 2002; Hudson and Mishra 2007). Therefore CCN from air pollution could be incorporated into orographic clouds and slow cloud-drop coalescence and riming on ice precipitation, hence delaying the conversion of cloud water into precipitation. The evidence includes significant decreasing trends of the ratio of hill / plains precipitation during the twentieth century in polluted areas. Aerosol measurements from the Interagency Monitoring of Protected Visual Environments (IMPROVE) aerosol monitoring network in the western United States showed that the negative trends in the orographic precipitation are associated with elevated concentrations of fine aerosols ( $PM_{2.5}$ ). No trends are observed in similar nearby pristine areas.

In Central California the main precipitation suppression is postulated to occur during westerly flow that ingests anthropogenic CCN, which are incorporated into orographic clouds that form over the Sierra Nevada and are so shallow that their tops do not fully glaciate before crossing the mountain crest. This means that at least some of the water in these clouds remains in the form of cloud droplets that are not converted to precipitation (or at least ice hydrometeors) before crossing the divide, and hence re-evaporate after producing some precipitation on the downwind side of the crest. Recent model simulations support this hypothesis (Lynn et al. 2007; Woodley Weather Consultants 2007). The worldwide evidence for the effect of aerosols on clouds and precipitation is summarized in Appendix A.



## 2.0 The SUPRECIP Program

Following the publication of many of the recent findings cited above the authors initiated a research effort called the Suppression of Precipitation (SUPRECIP) program to make in situ aircraft measurements of the polluting aerosols, the composition of the clouds ingesting them, and the way the precipitation-forming processes are affected. The SUPRECIP field campaigns were aimed at making the measurements necessary for the validation of the hypothesis that urban air pollution suppresses orographic precipitation.

SUPRECIP was conducted during February and March of 2005 (SUPRECIP-1) and February and March of 2006 (SUPRECIP-2). Operational documentation of SUPRECIP-2 is given in Appendix B. The Seeding Operations and Atmospheric Research (SOAR) Cheyenne II, turbo-prop, cloud physics research aircraft was used in SUPRECIP-1; the Cheyenne and an additional (SOAR) Cessna 340 aerosol aircraft were flown in SUPRECIP-2. Details about the SOAR aircraft and their instrumentation are given in Appendix C. These aircraft were used to measure (1) atmospheric aerosols in pristine and polluted clouds, and (2) the impact of the aerosols on cloud-base microphysics, the evolution with height of the cloud drop-size distribution, and precipitation development under warm and mixed-phase processes. The aircraft were used also to validate the multi-spectral satellite inferences of cloud structure and the effect of pollutants on cloud processes, especially the suppression of precipitation. This research effort is funded by the PIER (Public Interest Energy Research) Program of the California Energy Commission. Supplemental information about the SUPRECIP program is provided in the Appendices, including a complete treatment of the aircraft program.

Figure 1 shows the Cheyenne II cloud physics aircraft that was used in SUPRECIP. The instruments and respective data sets taken by the aerosol and cloud physics airplanes are given in Tables 1 and 2, respectively. These aircraft flights documented the aerosols and orographic clouds downwind of the densely populated areas in the north-central Sierra Nevada and contrasted them with the aerosols and clouds downwind of the sparsely populated areas in the far northern Sierra Nevada.



Figure 1. The SOAR Cheyenne II cloud physics aircraft

Table 1. Data sets from the aerosol aircraft

VARIABLE	INSTRUMENT	RANGE	ACCURACY	RESOLUTION	FREQUENCY
Air temperature	Rosemount 102DB1CB	-50°C to +50°C	0.1°C	0.01°C	1 Hz
Liquid water content	DMT LWC-100	0 to 3 g/m <sup>3</sup>	0.05 g/m <sup>3</sup>	0.01 g/m <sup>3</sup>	1 Hz
Logging, telemetry & event markers	ESD DTS (GPS)				1 Hz
Isokinetic aerosol inlet	Brechtel double diffuser inlet	28 lpm			100 m/s
Condensation nuclei (CN) concentration	TSI 3022A	>2 nm		0–105 cm <sup>-3</sup>	1 Hz
Cloud condensation nuclei (CCN)	DMT CCN counter	0.5 to 10 μm 0.1 to 1.2 % SS		0.5 μm, 20 bins	1 Hz

Note: Hz=hertz; g/m<sup>3</sup>=grams per cubic meter; lpm= liters per minute; m/s=meters per second; nm=nanometers; cm<sup>3</sup>=cubic centimeters; μm=micrometers; SS=supersaturation.

**Table 2. Data sets from the cloud physics aircraft**

VARIABLE	INSTRUMENT	RANGE	ACCURACY	RESOLUTION	FREQUENCY
Air temperature	Rosemount 102DB1CB	-50°C to +50°C	0.1°C	0.01°C	1 Hz
Air temperature (reverse flow)	0.038" DIA. Bead Thermistor	-30°C to +50°C	0.05°C/0.3°C incl DHC	0.01°C	< 1 s TC
Relative humidity (reverse flow)	Thermoset Polymer RH Sensor	0 to 100% RH	2% RH	0.1% RH	5 s TC @ 20°C
Barometric pressure	MEMS Pressure Sensor	0 to 110000 Pa	100 Pa	10 Pa	20 Hz
u wind component (+ North)	Extended Kalman Filter (EKF)		0.50 m/s @ 75 m/s TAS	0.01 m/s	5 Hz
v wind component (+ East)	Extended Kalman Filter (EKF)		0.50 m/s @ 75 m/s TAS	0.01 m/s	5 Hz
w wind component (+ Down)	Extended Kalman Filter (EKF)		0.50 m/s @ 75 m/s TAS	0.01 m/s	5 Hz
Position (Latitude/Longitude)	WAAS DGPS		2 m (2 $\sigma$ )	< 1 m	5 Hz
Altitude	WAAS DGPS	-300 to 18000 m	5 m (2 $\sigma$ )	< 1 m	5 Hz
Geometric Altitude	King KRA 405 Radar Altimeter	0 to 2000 ft	3% < 500 ft 5% > 500 ft	0.48 ft (0.15 m)	
Roll Attitude ( $\phi$ )	MEMS IMU/GPS/EKF	-60 to +60°	0.1°	0.01°	5 Hz
Pitch Attitude ( $\theta$ )	MEMS IMU/GPS/EKF	-60 to +60°	0.2°	0.01°	5 Hz
Yaw Attitude ( $\psi$ )/ Heading	MEMS IMU/GPS/EKF	0 to 360°	0.1°	0.01°	5 Hz
Angle of attack ( $\alpha$ )	MEMS Pressure Sensor	-15 to +15°	0.03° @ 150 m/s	0.001° @ 150 m/s	20 Hz
Side-slip ( $\beta$ )	MEMS Pressure Sensor	-15 to +15°	0.03° @ 150 m/s	0.001° @ 150 m/s	20 Hz
True Air Speed	MEMS Pressure Sensor	0 to 150 m/s	0.1 m/s	0.01 m/s	20 Hz
Logging, telemetry & event markers	ESD DTS (GPS)				1 Hz
Cloud droplet spectra	DMT CDP	2 to 50 $\mu\text{m}$		1 to 2 $\mu\text{m}$ , 30 bins	1 Hz
	PMS FSSP SPP-100	2 to 47 $\mu\text{m}$		1 to 2 $\mu\text{m}$ , 30 bins	1 Hz
Cloud particle spectra	DMT CIP 1D	25 to 1550 $\mu\text{m}$		25 $\mu\text{m}$ , 62 bins	1 Hz
Cloud particle image	DMT CIP 2D	25 to 1550 $\mu\text{m}$		25 $\mu\text{m}$	
Liquid water content	DMT LWC-100	0 to 3 g/m <sup>3</sup>	0.05 g/m <sup>3</sup>	0.01 g/m <sup>3</sup>	1 Hz
	CDP calculated	> 3 g/m <sup>3</sup>			1 Hz
	FSSP calculated	> 3 g/m <sup>3</sup>			1 Hz
CN concentration	TSI 3010	>7 nm		0–105 /cm <sup>3</sup>	1 Hz

Note: DHC=Dynamic Heating Correction; Pa=pascals; TAS=True Air Speed; CDP=Cloud Droplet Probe; CIP= Cloud Imaging Probe; FSSP=Forward Scattering Spectrometer Probe.

## 2.1. The SUPRECIP-1 Effort

The focus of SUPRECIP was on the nature and source of the pollution aerosols that ancillary analyses had suggested were decreasing the orographic component of precipitation in the California Sierra Nevada. These aerosols are tiny CCN. High CCN concentrations reduce droplet sizes and thus inhibit precipitation-forming coalescence processes and ultimately the riming of ice crystals. According to the satellite inferences, the decreases in  $r_e$  are taking place over the central and southern Sierra where the losses in precipitation and stream flows have been documented (Woodley Weather Consultants 2005) but not in the far northern Sierra, where no such changes were noted. The primary motivation for the SUPRECIP-1 project was to determine whether the satellite-inferred cloud properties, especially the  $r_e$ , could be validated by actual measurements taken by a cloud physics aircraft within the subject clouds.

The weather during SUPRECIP-1 was highly anomalous for the entire U.S. West Coast, with dry conditions in the Pacific Northwest and flooding rains in Southern California. A high-pressure blocking pattern at the surface and aloft tended to split the jet-stream flow to the north or south of the northern Sierra. This persistent region of low pressure under the block produced southerly and southeasterly winds and long periods of middle and high clouds over the Central and Northern Sierra for most of the project. The desired orographic clouds produced by the usual westerly winds into the Sierra were a rarity during SUPRECIP-1. Therefore, the program was extended through the first week in March.

Use of the Cheyenne II turbo-prop cloud-physics aircraft enabled researchers to document differences in cloud microphysics associated with differences in CCN that were visibly related to air pollution. It was determined that these differences were consistent with satellite retrievals—a crucial finding, because previously only the satellite retrievals were available as indicators of the apparent negative effect of pollution on Sierra precipitation, as published initially for Australia (Rosenfeld 2000) and later for the Sierra (Woodley Weather Consultants 2007). Thus, the new aircraft measurements could be used to validate the satellite inferences of cloud microphysics, using the method described in Appendix D, by showing the negative impact of pollutants on cloud processes and precipitation. The aircraft and satellite measurements in SUPRECIP showed that some of the Sierra precipitation was produced by surprisingly shallow pristine clouds. This evidence suggested that pollution may help explain the long-term losses in Sierra orographic precipitation.

To provide better comparisons with aircraft data, satellite inferences of  $r_e$  were made for cloud pixels in a series of boxes that encompassed portions of the aircraft flight tracks. These provided comparisons of aircraft -and satellite-derived median  $r_e$  for the cloud passes at the height and temperature of each pass. The results are given in Figure 2, which shows a scatter plot of  $r_e$  measured by the cloud physics aircraft versus the inferences of  $r_e$  from the satellite imagery (Satellite median  $r_e$ ) for two SUPRECIP-1 study days. Considering the differences in scale (i.e., individual cloud passes versus the composite clouds within a box that contains the cloud passes) and time, the agreement is reasonable (linear correlation = 0.73). The California regions that experienced losses in precipitation and stream flow had decreased  $r_e$  values compared to those for more pristine California areas. Although it seemed reasonable to ascribe the decreased droplet sizes to the ingestion of pollution aerosols, such causality had not been proved.

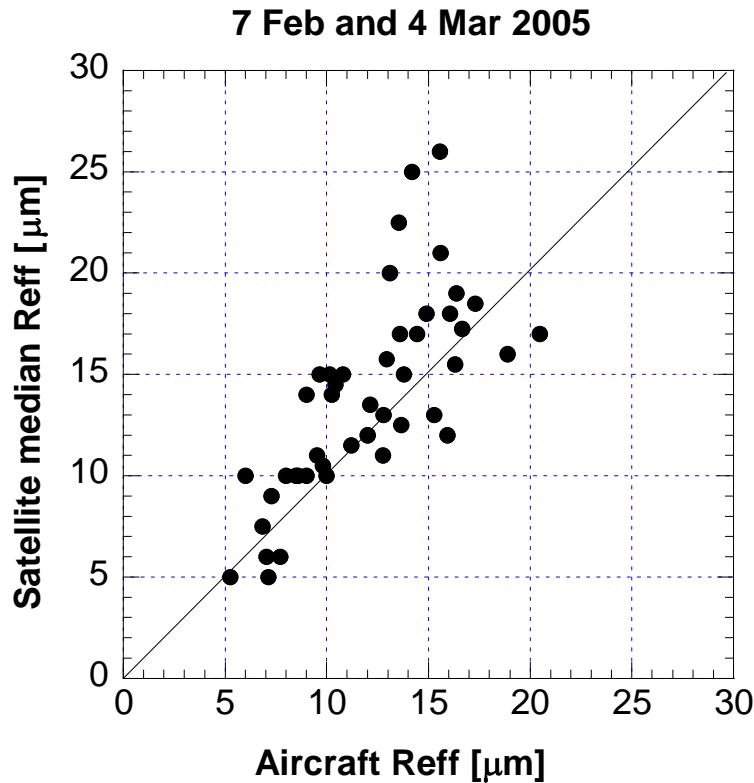


**Figure 2. Scatter plot of the median effective radii ( $r_e$ ) determined by aircraft (Aircraft  $r_e$ ) for individual cloud passes vs. the median  $r_e$  inferred from the multi-spectral satellite imagery (Satellite median  $r_e$ ) for the altitudes and temperatures of the aircraft cloud passes for clouds in regions where the cloud passes were made. The comparisons were made for data obtained on February 7 and March 4, 2005.**

Additional analyses were made for those days with complete cloud microphysical data sets, including time, altitude and temperature of the cloud passes, the cloud droplet probe (CDP), liquid water content (LWC), mean and maximum droplet concentrations, and median  $r_e$  for each cloud pass. The cloud imaging probe (CIP) instrument provided an estimate of the precipitation water. Aerosol information was supplied by a CCN counter operated at 0.5% supersaturation (SS). The total aerosols as a function of size were provided by Texas A&M University's aircraft-based high flow rate Differential Mobility Analyzer (DMA)/Tandem Differential Mobility Analyzer (TDMA).

The SUPRECIP-1 data were used to show an association between the CCN concentrations and the in-cloud droplet concentrations before and after each cloud pass at the same altitude. Figure 3 shows a scatter plot and regression analysis of in situ droplet concentrations (mean and maximum) and CCN concentrations—before and after the cloud penetrations at the same altitude. This figure shows that the greater the CCN concentration around the cloud, the greater the in-cloud droplet concentrations. Thus, aerosols would appear to have a direct effect on in-cloud microphysics.

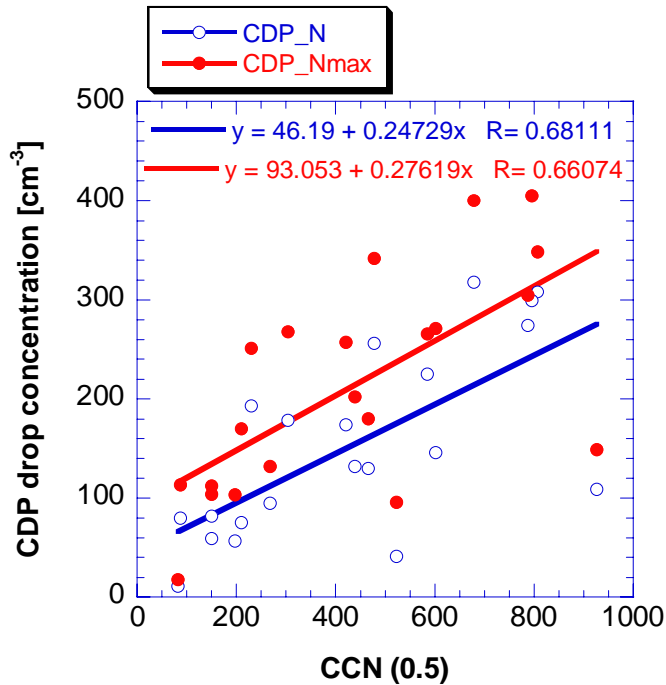


**Figure 3. Cloud drop number concentrations as a function of the CCN concentration before and after cloud pass at a supersaturation of 0.5%. Each point represents the median (blue) and maximum (red) droplet concentrations for one cloud pass. The best-fit equations are as shown.**

The next step was to relate the CCN concentrations to the effective diameter ( $De_{eff}$ ) of the cloud droplets. This requires normalization to the cloud LWC with the expression  $De_{eff} / LWC^{0.333}$  for each cloud pass. This normalization is needed because  $De_{eff}$  and LWC generally increase with distance above cloud base. Variations in cloud-penetration distances above cloud base need to be accounted for to make valid comparisons with CCN. The ratio with LWC is used because cloud base height and/or distance from cloud base is seldom known.  $LWC^{0.33}$  is used because this is generally proportional to  $De_{eff}$  (droplet diameter relates to the cube root of the volume). The CCN concentrations were taken from the immediate clear air vicinity of the cloud passes. The negative relationship is given by the regression equation. Figure 4 shows that  $De_{eff}$  decreases as the CCN concentration increases. Thus, air pollution CCN decrease cloud droplet sizes.

In summary, the flights of SUPRECIP-1 documented the aerosols and orographic clouds in the central Sierra Nevada and contrasted them with the aerosols and clouds downwind of the sparsely populated areas in the northern Sierra Nevada. The main results from SUPRECIP-1 (Woodley Weather Consultants 2005) are as follows:

- The in situ aircraft measurements of the cloud microphysics validated the satellite retrievals of  $r_e$  and microphysical phase.



- Ample supercooled drizzle drops were found in the pristine orographic clouds with only few tens of drops  $\text{cm}^{-3}$ , and no drizzle with small concentrations of graupel were found in clouds with drop number concentrations of approximately  $150 \text{ cm}^{-3}$ .
- The pristine clouds occurred in air masses that were apparently decoupled from the boundary layer in the early morning, whereas the more microphysically continental clouds occurred during the afternoon after the surface inversion over the Central Valley disappeared.

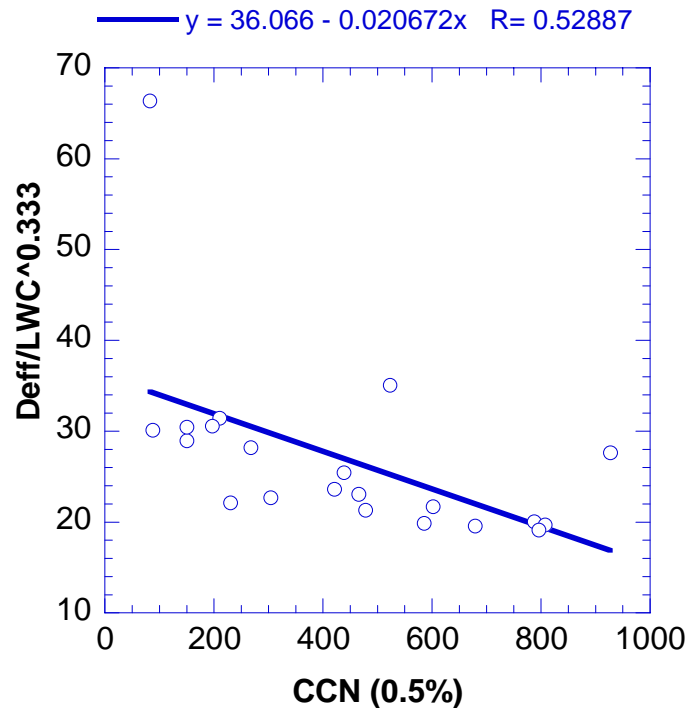


**Figure 4. The effective diameter ( $D_{eff}$ ) of the cloud drops normalized to the cloud liquid water content (LWC) by the expression  $D_{eff} / LWC^{0.333}$ , as a function of the CCN concentrations for each cloud pass**

Despite the accomplishments of SUPRECIP-1, all of its objectives had not been met because of incomplete documentation of the aerosols in the atmospheric boundary layer, due to the near impossibility of obtaining clearance to conduct flight under instrument flight rules (IFR) in the boundary layer in the San Francisco/Oakland/Sacramento heavily populated urban and industrial areas. A second aircraft flying under visual flight rules (VFR) would have been necessary to obtain the needed documentation. In addition, the lack of orographic cloud conditions over the California Sierra Nevada due to weak wind flow into the Sierra during virtually all of the period of flight operations was a major problem. A longer period of operations would have been required to obtain the desired orographic clouds.

## 2.2. The SUPRECIP-2 Effort

A second field campaign (SUPRECIP-2) was conducted in February and March 2006 to better document the aerosol effect on clouds. The cloud physics instrumentation was enhanced with another cloud droplet spectrometer (FSSP SPP-100), and a second low-level aerosol airplane was added. Two research aircraft were involved, making measurements of CCN, condensation nuclei (CN),<sup>1</sup> cloud drop size distribution, hydrometeor images and size distributions, the thermodynamic properties of the air, and air three-dimensional winds. Information about the CN and CCN instrumentation on the aerosol aircraft and the CN instrument on the cloud physics aircraft is provided in Tables 1 and 2, respectively. SUPRECIP-2 was augmented also by surface measurements of aerosols and chemical composition of the hydrometeors, made by collaborating research groups from the Desert Research Institute of the University of Nevada, the University of California (UC) Davis, and the SCRIPPS Oceanographic Institute of UC, San Diego. This effort provided coincident measurements of the low-level aerosols and the properties of the clouds that ingest them. The results reported here confirm the link between anthropogenic aerosols and the suppression of precipitation-forming processes in California clouds.

The aerosol aircraft operated below the bases of the clouds that the cloud physics aircraft monitored, which provided measurements of the aerosol that was ingested into these clouds. The SUPRECIP-2 project's goal was to measure atmospheric aerosols in pristine and polluted clouds and document the effect of the aerosols on cloud-base microphysics, on the evolution with height of the cloud drop-size distribution and on the development of precipitation under warm and mixed-phase processes. The objectives in the context of this goal included the following:

- Systematically “mapping” the pollution aerosols at low to mid levels in urban and downwind areas using both research aircraft.
- Documenting the connection between the aerosols and the measured cloud microphysics and precipitation forming processes.
- Validating the multi-spectral satellite inferences of cloud structure and the effect of pollutants on cloud processes, especially precipitation suppression.

During the SUPRECIP-2 project, the research team flew 53 research missions—25 with the cloud physics aircraft and 28 with the Cessna 340 aerosol aircraft. A little over half (27 of 53) of the research missions were flown in March 2006, when the weather was much more favorable (10 flight days) than it was in February. Appendix B provides additional operational details.

---

<sup>1</sup> The CN measurement expresses the total aerosol present at the sampled location.

### 3.0 Results of SUPRECIP-2 Analyses

#### 3.1. Establishing a Direct Link Between the Sub-Cloud Aerosols and Cloud Microphysical Structure

##### 3.1.1. A Case Study: February 28, 2006

The linkage between ingested sub-cloud aerosols and cloud microphysics is best illustrated by a case study from the afternoon of February 28, 2006. A cold front had passed through the area the previous night and a post-frontal cold air mass moved from the west southwest over all of Central California by the following afternoon. Post-frontal instability caused convective clouds over the ocean and triggered convective clouds over the coastal hills and the Sierra Nevada. Although the instability decreased gradually during the day, rain showers from shallow clouds were still occurring over the ocean and the coastal ranges at 00Z on March 1, 2006. Figure 5 shows the Oakland rawinsonde at that time.

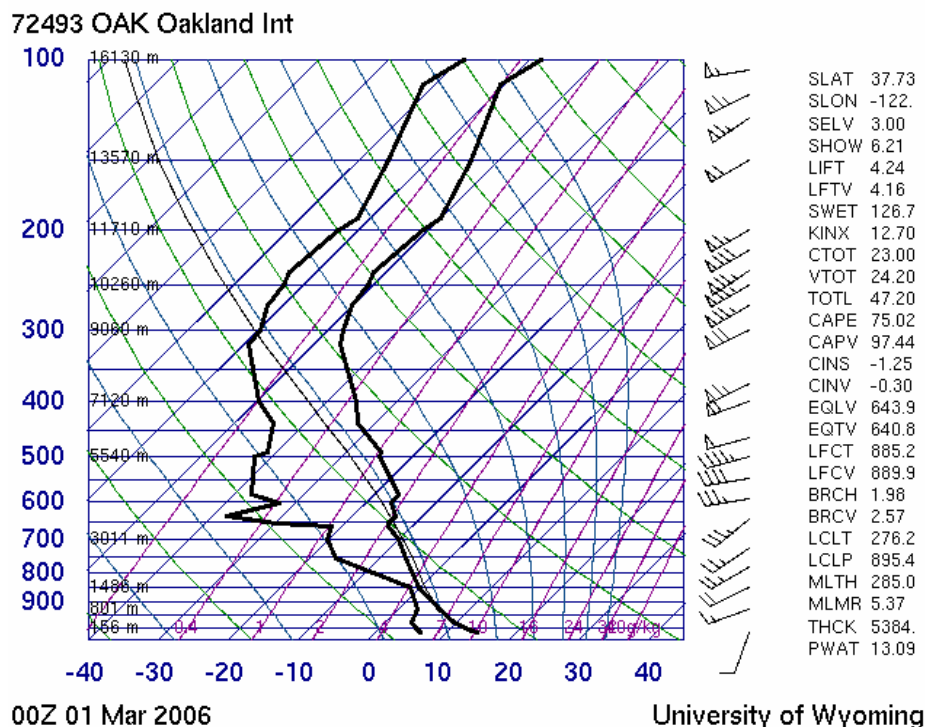
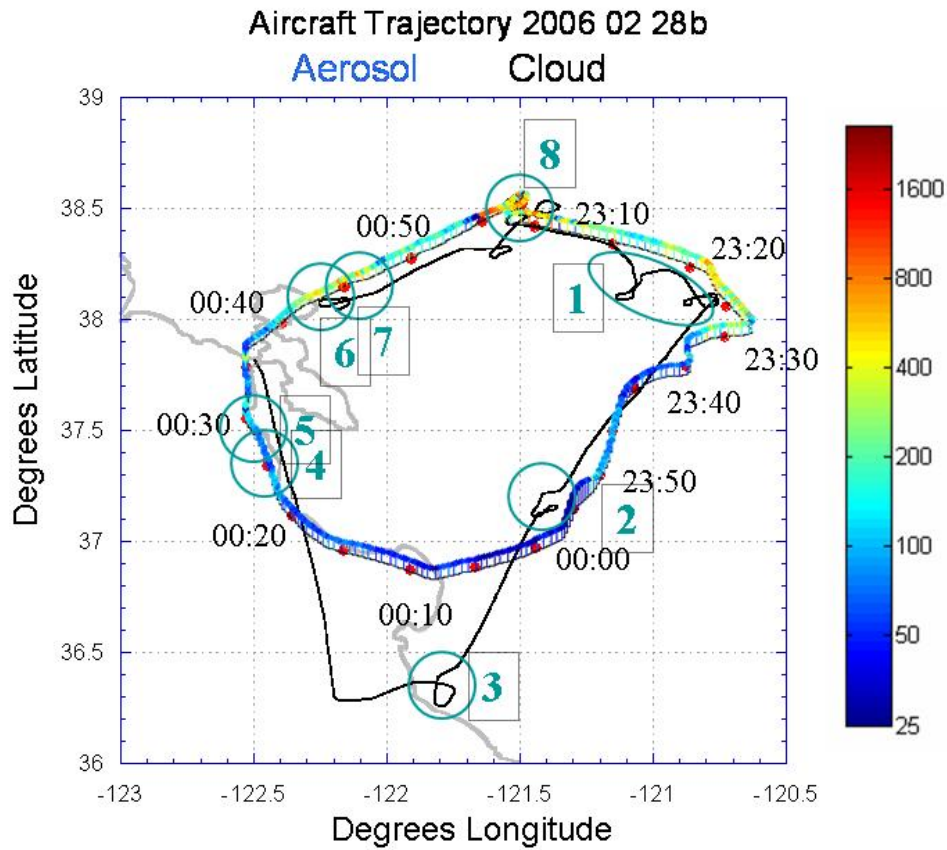


Figure 5. The Oakland rawinsonde of March 1, 2006, at 00Z, which is near the time that the aircraft flew near Oakland

A coordinated mission of the Cloud and Aerosol airplanes originated from Sacramento Executive Airport to document the gradient in aerosols and cloud properties by flying cross sections from the Sierra Nevada to and from the Pacific Ocean. The aircraft departed Sacramento at 23:05Z and flew due east to the foothills, where from 23:20Z to 23:30Z it measured the convection generated there by the mountains. The next destination was the clouds that formed over the hills bounding the Central

Valley to its west, about 60 kilometers (km) to the northeast of Monterey. Next the aircraft sampled the clouds forming over the hills just at the Pacific coast at Big Sur. There the aircraft continued 35 km westward over the ocean and then turned north to measure convective clouds that were triggered by the ocean shoreline of San Francisco. Then the aircraft turned east over the north part of San Francisco Bay and measured a cloud just inland over Richmond, and then another cloud over Sacramento before finally landing. Figure 6 provides the tracks of the two aircraft and the locations of the measured clouds.



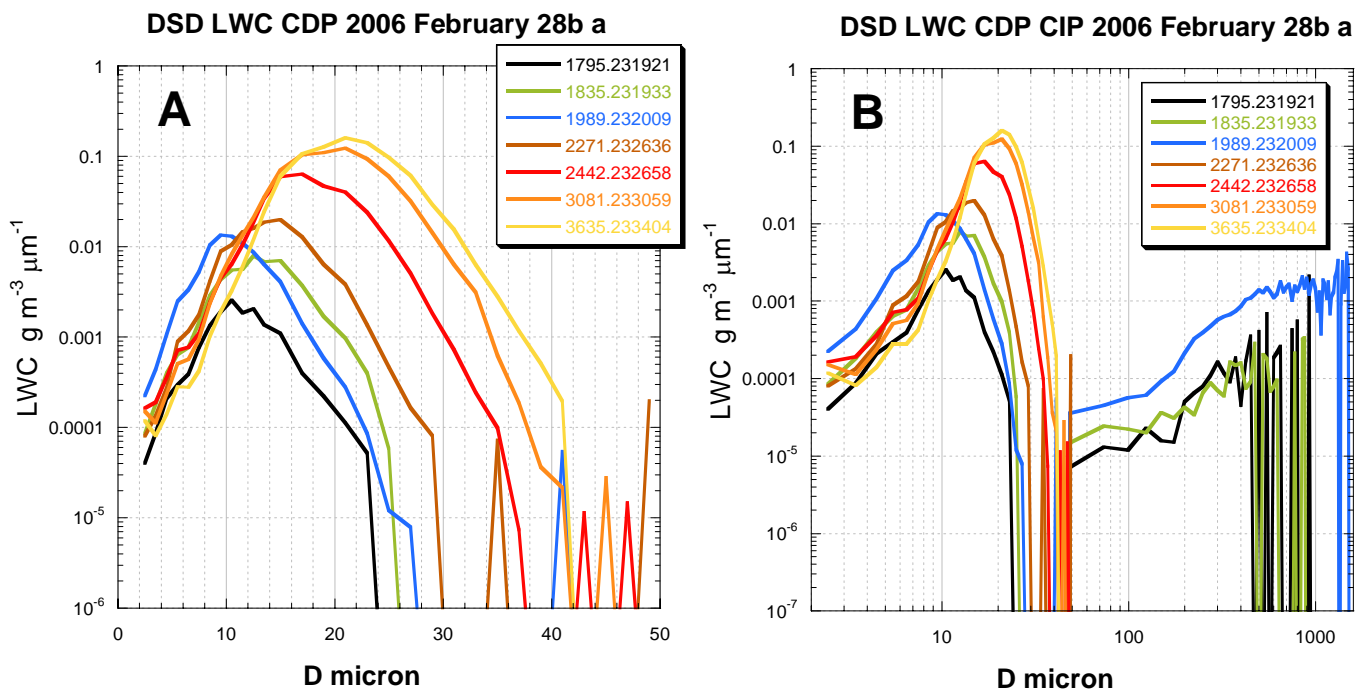
**Figure 6. The tracks of the Cloud (black) and Aerosol (colored) airplanes. The time marks every 5 minutes are posted on the aerosol aircraft tracks and labeled every 10 minutes. The CCN concentrations adjusted to supersaturation of 0.9% are shown in the color scale. The relative height of the aerosol aircraft above sea level is shown by the vertical displacement of the track. The clouds measured by the cloud physics aircraft are marked with green circles and numbered sequentially.**

Figure 6 also summarizes the aerosol aircraft measurements. Because the supersaturation (SS) caused by the temperature difference between the plates ( $dT$ ) in the Cloud Condensation Nuclei Counter cycles approximately every seven minutes, there was a need to correct the CCN data measured at low supersaturations to a common SS. Without correction or adjustment there would be too few data points measured at the same SS. To correct the data, it was necessary to find the relation between  $dT$  (instead of SS) and the CCN concentration for each flight separately, because this relation might be affected by the chemical composition of the aerosols, their sizes, and their concentrations. After determining and applying the correction, the CCN concentrations were plotted for an entire flight to a common 0.85% SS for measurements in the boundary layer.

The aircraft aerosol measurements show CCN concentrations varying between 300 and 800  $\text{cm}^{-3}$  over the first section to the southeast at the western slopes of the Sierra Nevada. The CCN concentrations fell to about 100  $\text{cm}^{-3}$  over the hills 60 km northeast of Monterey, and continued falling to less than 40  $\text{cm}^{-3}$  over Monterey Bay and likely also over Big Sur. The CCN increased again gradually to the north along the coastline and reached about 70  $\text{cm}^{-3}$  there. They kept rising to about 100  $\text{cm}^{-3}$  over the peninsula of San Francisco airport and jumped locally to 800  $\text{cm}^{-3}$  just north of the airport, but recovered back to less than 80  $\text{cm}^{-3}$  north of the Golden Gate Bridge. The aircraft turned east and experienced a sharp increase of the CCN to more than 700  $\text{cm}^{-3}$  over Richmond. The condensation nuclei (CN) then shot up  $> 10,000 \text{ cm}^{-3}$ . This suggests an ample source of fresh small aerosols. The CCN remained generally above 500  $\text{cm}^{-3}$  within the boundary layer all the way to landing in Sacramento.

The cloud and precipitation particle size distributions are given in Figures 7-11. Cloud 1 was sampled stepping upward from base through its upshear towers, whereas its more mature portions glaciated and precipitated. Due to air traffic control limitations it was necessary to use different clouds in the same area for the lower and upper portions of the cross sections. The modal liquid water cloud drop diameter (DL, defined as the drop diameter having the greatest LWC) increased with height above cloud base. It reached 21 micrometers ( $\mu\text{m}$ ) at the altitude of 3635 meters (m), which is about 1900 m above cloud base. The temperature there was  $-8^\circ\text{C}$ . This size is below the threshold for DL for the development of warm rain that was documented elsewhere as 24  $\mu\text{m}$  (Andreae et al. 2004). In agreement with that, the DL did not expand to drizzle size. Large precipitation particles occurred as graupel and formed a well-separated distribution at the 1 millimeter (mm) size range (Figure 7).

From the location of Cloud 1 the aircraft was flown diagonally to the southwest and across the Central Valley. The valley was mostly cloud-free, except for some mid-level layer clouds. The next area of clouds was triggered by the ridge that bounds the Central Valley on its west. The cloud tops had a convective appearance and were sampled at the lowest allowed altitude (2100 m, to provide safe-ground clearance over the highest terrain) up to the cloud tops at 2700 m. The temperature there was  $-3^\circ\text{C}$ , but the maturing clouds were visibly glaciating, probably by a mechanism of ice multiplication. The modal LWC drop size was 28  $\mu\text{m}$  at 2100 m and reached 33  $\mu\text{m}$  at the cloud top at 2700 m. This is clearly beyond the threshold (DL = 24  $\mu\text{m}$ ) for warm rain (Gerber 1996; Yum and Hudson 2002). In agreement with that, the cloud droplet size distribution (DSD) was extended smoothly to the drizzle and small rain drop sizes, as measured by the CIP and presented in panel B of Figure 8. The appearance of the warm rain is consistent with the decrease of the CCN concentrations to about 100  $\text{cm}^{-3}$ .



**Figure 7. Plot of cloud droplet diameters as a function of liquid water content (LWC) for Cloud 1 over the western slopes of the Sierra Nevada (see location in Figure 6). The modal liquid water drop diameter occurs at the droplet size having the greatest water content. Cloud 1 developed in an air mass that had 300–800 CCN cm<sup>-3</sup>. Panel A shows the Cloud Droplet Probe (CDP)-measured LWC distribution. Each line represents the gross cloud drop size distribution of a whole cloud pass. The legend of the lines is composed of the pass height [m] to the left of the decimal point, and the pass starting GMT time [hhmmss] to the right of the point. The passes are ordered in altitude ascending order. Note the increase in cloud drop volume modal size with increasing cloud depth. Panel B shows the combined distributions of the CDP and the cloud imaging probe (CIP). According to the figure the large precipitation particles were well separated from the cloud drop size distribution, indicating lack of appreciable coalescence.**

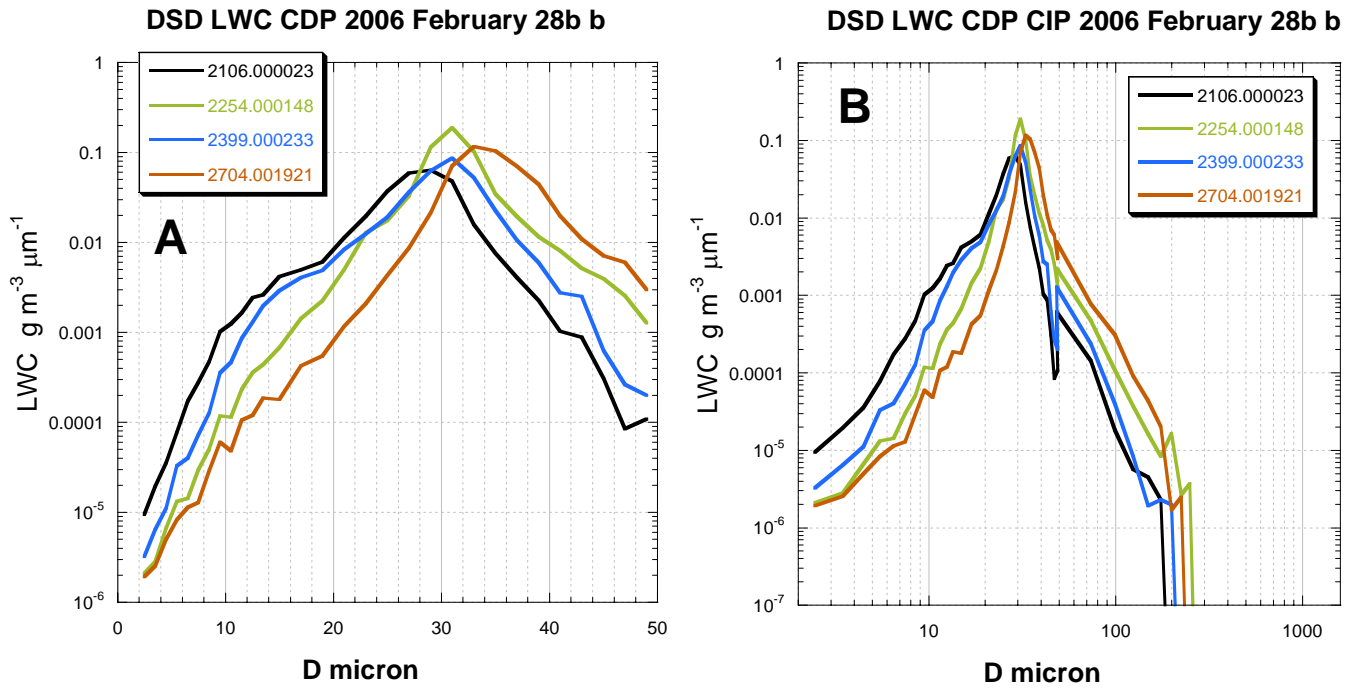


Figure 8. Same as Figure 7, but for Cloud 2 over the hills 60 km NE of Monterey (see location in Figure 6). It developed in an air mass that had  $100 \text{ CCN cm}^{-3}$ . The cloud drops are quite large and the distribution continues smoothly into the rain drop sizes. This indicates active warm rain processes.

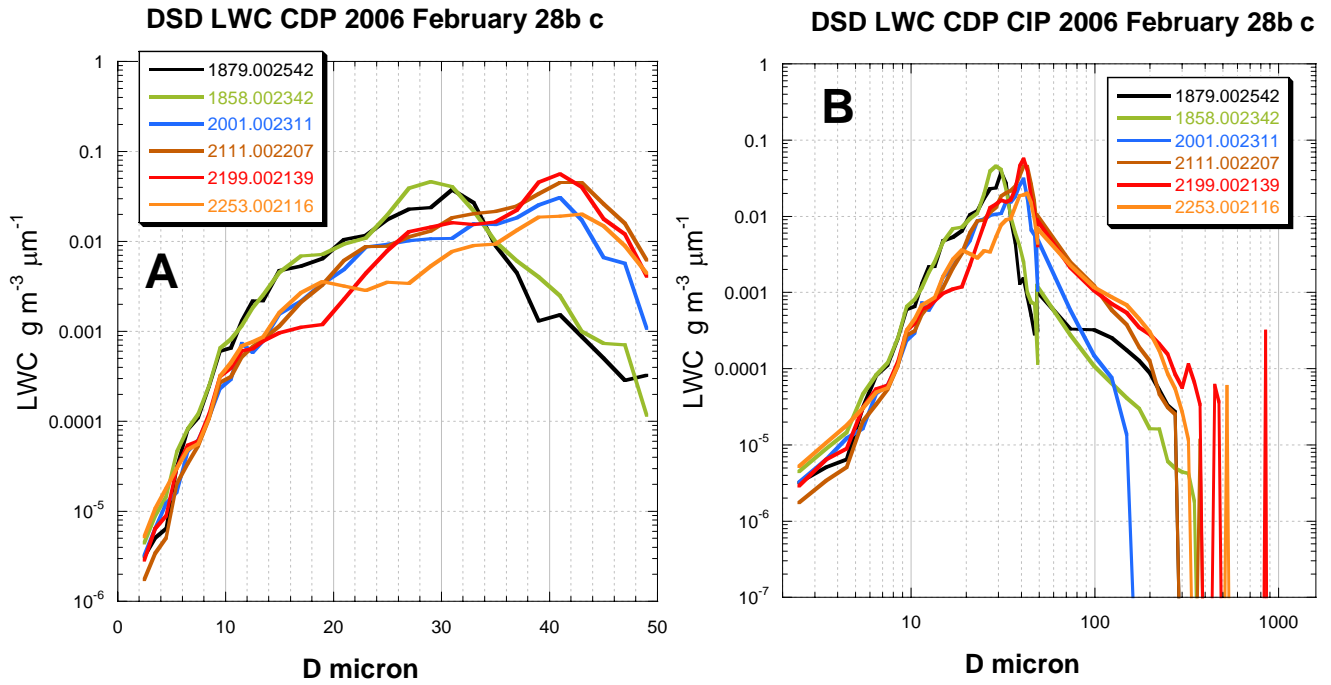


Figure 9. Same as Figure 7, but for Cloud 3 over the hills near Big Sur (see location in Figure 6). It developed in an air mass that had about  $40 \text{ CCN cm}^{-3}$ . The cloud drops are very large, and the distribution continues smoothly into the rain drop sizes. This indicates very active warm rain processes.



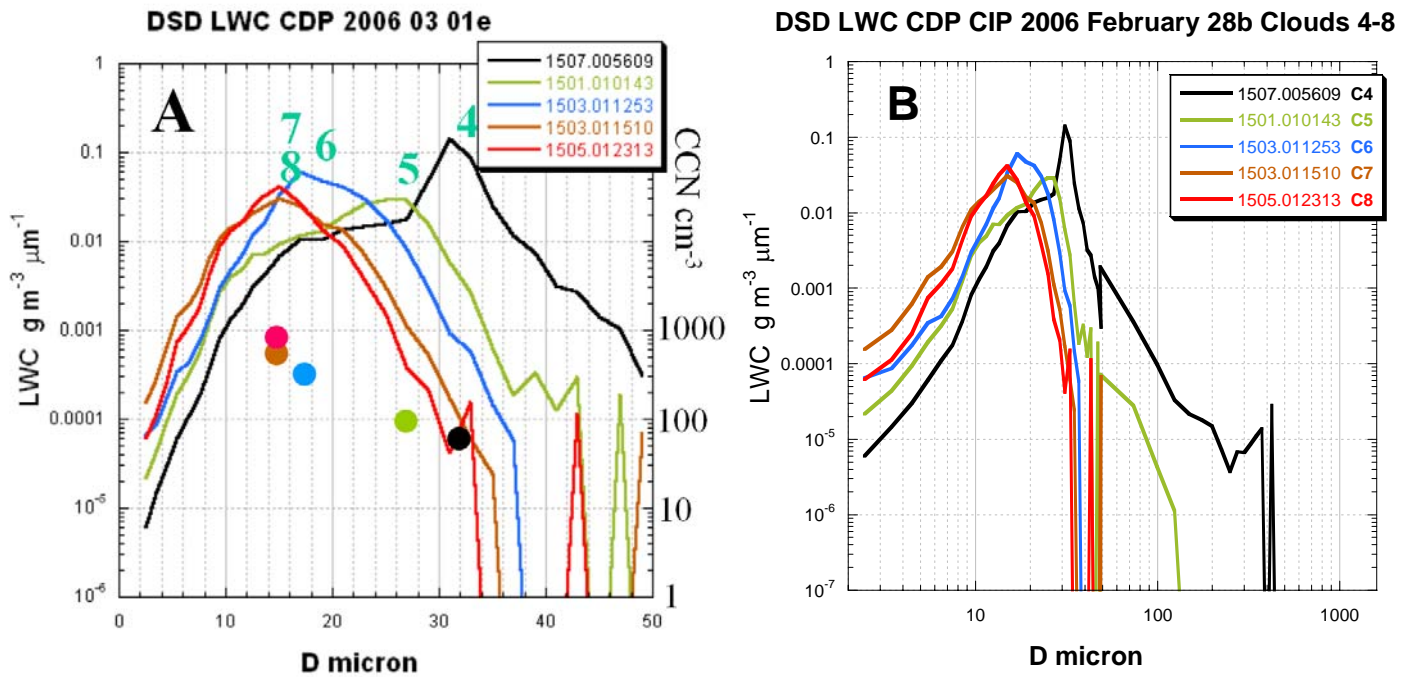


Figure 10. Same as Figure 7, but for single heights in clouds 4–8 in a cross-section from the Pacific Ocean to Sacramento, marked by clouds 4, 5, 6, 7, and 8, respectively. The respective approximated CCN concentrations from the measurements made by the aerosol aircraft are denoted by the circles and are located under the peaks of the DL plots having the same color. The CCN values are to be read from the right ordinate. The CCN concentrations are: Cloud 4: 70; Cloud 5: 100; Cloud 6: 300; Cloud 7: 600; Cloud 8: 800  $\text{cm}^{-3}$ . The drops become markedly smaller with increasing CCN concentrations. Warm rain ceases at Cloud 3, where 300  $\text{CCN cm}^{-3}$  were present.

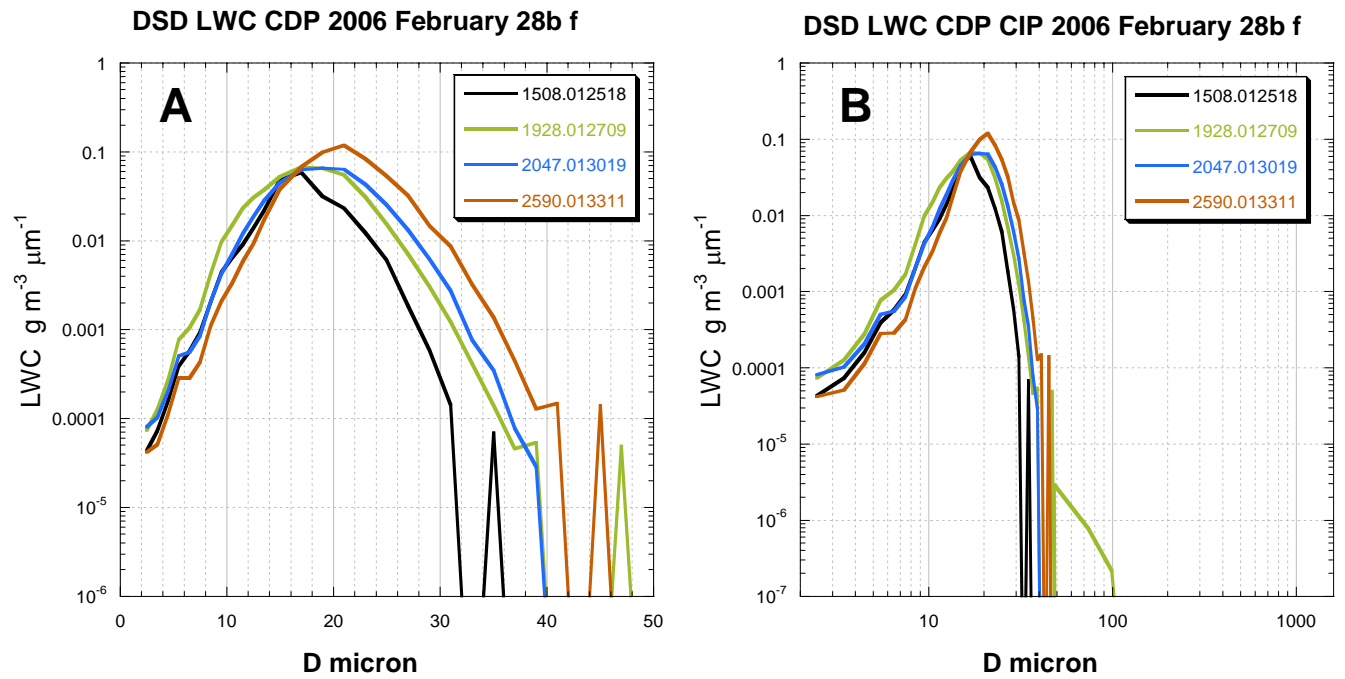


Figure 11. Same as Figure 7 but for the vertical cross-section in Cloud 8 over Sacramento (see location in Figure 6). It developed in an air mass that had about  $800 \text{ CCN cm}^{-3}$ . The cloud drops are very small and do not expand much with height into raindrops, again as in Cloud 1.

The aircraft continued flying to the southwest to the next area of clouds (Cloud 3). These were triggered by the coastal hills near Big Sur. The aircraft stepped vertically through the convective-looking cloud tops from the lowest safe height of 1880 m to their tops at a height of 2250 m at a temperature of  $-3^{\circ}\text{C}$ . The CCN concentrations as measured by the aerosol aircraft in Monterey Bay varied between 20 and  $50\text{ cm}^{-3}$ . These low CCN concentrations produced large cloud drops ranging from a modal LWC drop diameter of  $30\text{ }\mu\text{m}$  at 1880 m to  $43\text{ }\mu\text{m}$  at the cloud tops. The DSD extended smoothly into drizzle and small rain drops (see Figure 9). Large hydrometeors were nearly absent. The cloud drops were so large so that the solar radiation reflected from the particles near the cloud top formed a cloud bow. These clouds had clearly created active warm rain.

From Big Sur the flight continued over the ocean and then turned north and flew at a constant altitude across Monterey Bay to the Golden Gate and then eastward back to Sacramento. This flight path took the aircraft along an aerosol gradient that increased from pristine over the ocean to polluted air just to the east of San Francisco Bay. Convective clouds grew along that flight path and reflected the impact of the changing CCN concentrations at that fixed altitude. Clouds 4 to 8 were penetrated along this gradient flight (Figure 10).

Cloud 4 was penetrated at the coastline of the peninsula to the west of San Francisco. The CCN concentration there was about  $70\text{ cm}^{-3}$  and the cloud had a DL of  $31\text{ }\mu\text{m}$  and created warm rain. A faint cloud bow was barely visible. Cloud 5 was penetrated a short distance to the north, where the CCN increased to  $100\text{ cm}^{-3}$ . Cloud 5 still had warm rain, but to a lesser extent than Cloud 4. Shortly after passing directly over San Francisco International airport, over the Golden Gate Bridge, a short jump in the CCN occurred to about  $600\text{ cm}^{-3}$  and recovered to the background of  $< 70\text{ cm}^{-3}$ .

The aircraft turned east and crossed the northern arm of San Francisco Bay. The CCN concentrations increased to about  $300\text{ cm}^{-3}$  shortly after crossing the coast line. Cloud 6 formed over the eastern part of Richmond. Its modal LWC DSD decreased to  $17\text{ }\mu\text{m}$ , well below the warm rain threshold of  $24\text{ }\mu\text{m}$ . The CIP confirmed that this cloud had no precipitation particles. The CIP readings occurred less than an hour after the time of the Oakland sounding at 00Z, which represented pretty well the local conditions and showed light southwesterly winds near the surface that veered to stronger west-southwest wind at the higher levels.

Cloud 7 occurred a few km farther east of Cloud 6, where the CCN concentrations increased to  $600\text{ cm}^{-3}$ . Its DL decreased further to  $15\text{ }\mu\text{m}$ . Cloud 8 developed farther east over Sacramento, where the CCN concentration varied between 600 and  $1000\text{ cm}^{-3}$ . The cloud had a similar microphysics to Cloud 7. A vertical stepping through cloud 8 showed little widening of the DSD with height (Figure 11), which serves as an additional indication of the coalescence scarcity in that cloud.

A satellite analysis (Figure 12) shows that the satellite-retrieved microphysics of the cloud field is in agreement with the in situ measurements that suggest suppression of precipitation in Area 1 (which includes Cloud 1) while showing ample warm rain in Area 8 (which includes Cloud 3).

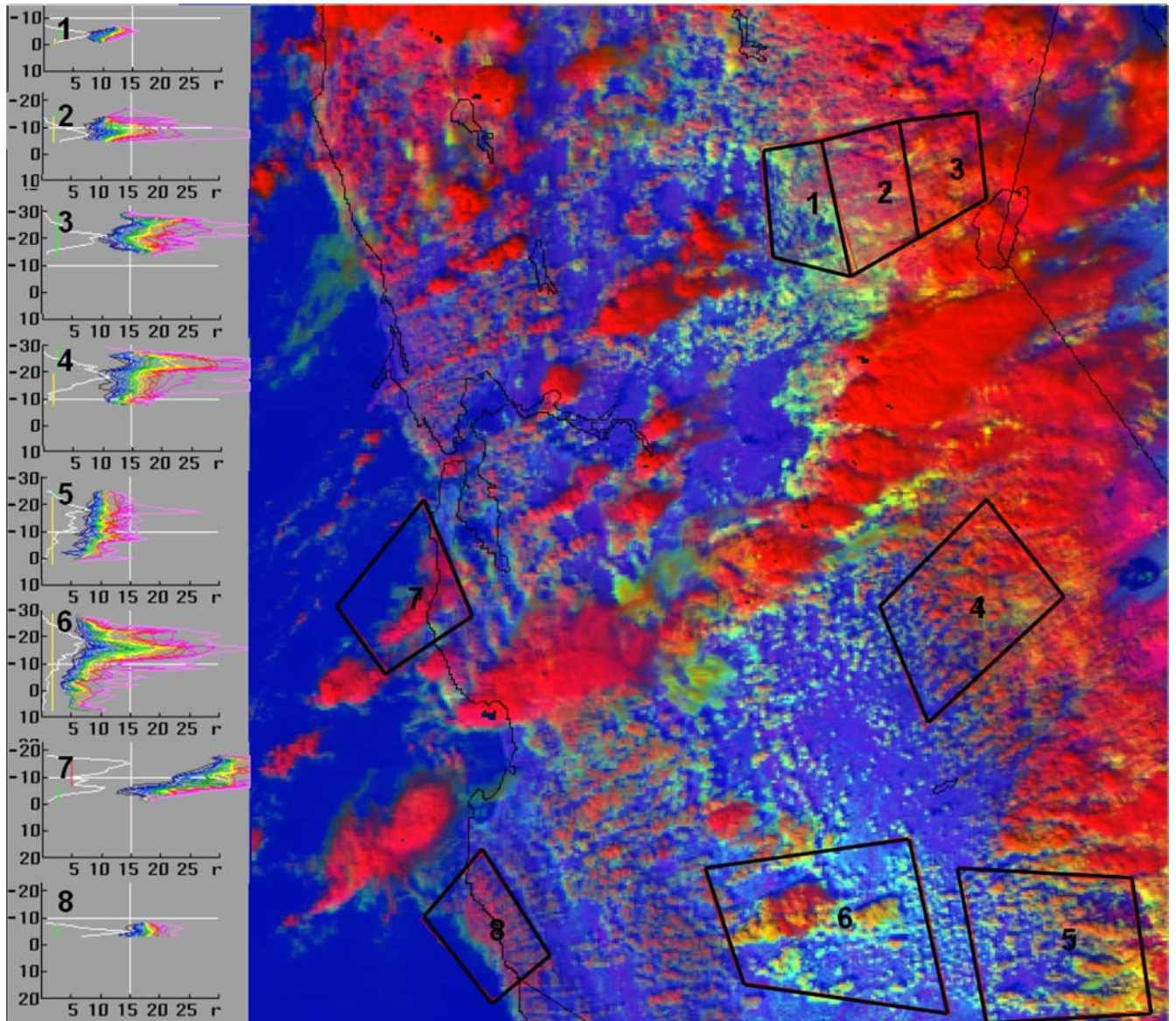


**Figure 12.** An image from the MODIS on NASA's Aqua satellite of the clouds in Central California on February 28, 2006, at 21:00Z. The color scale is a composite following Rosenfeld and Lensky (1998) where the red is modulated by the visible solar reflectance, blue modulated by the thermal temperature, and green modulated by the  $3.7 \mu\text{m}$  solar reflectance component. The green is brighter for smaller cloud particles. Therefore, the polluted clouds with small drops appear yellow (see Areas 1, 5 and 6); whereas the ice clouds appear red (see areas 3 and 7). Pristine water clouds appear magenta (see Area 8), because they have low green (large water drops) and high blue (warm temperature). The line graphs provide the relations between the satellite-indicated cloud top temperatures and the cloud top particle effective radii. At the foothills in Areas 1 and 5 the cloud top effective radius is much smaller than the precipitation threshold of  $14 \mu\text{m}$  (Rosenfeld and Gutman 1994), whereas the effective radius of  $18 \mu\text{m}$  in Area 8 is much larger than the precipitation threshold.

In summary, a detailed analysis of a single flight of SUPRECIP-2 showed a clear relationship between CCN concentrations, cloud microphysics, and precipitation-forming processes. The distribution of the CCN showed an unambiguous urban source, at least in the San Francisco Bay Area. The role of the anthropogenic aerosols is demonstrated by the contrast between Cloud 2 some 50 km inland in a relatively sparsely populated area, compared with clouds 6 and 7 only several kilometers inland over the heavily populated and industrialized Bay Area. Although Cloud 2 was quite pristine and produced ample coalescence and warm rain, coalescence in Cloud 7 was highly suppressed, and it produced no precipitation. The satellite image (Figure 12), taken three to four hours before the flight, supports the aircraft observations and shows that an even greater source than the urban San Francisco Bay Area occurred in the central and southern Central Valley. A flight earlier in the day measured CN concentrations exceeding  $20,000 \text{ cm}^{-3}$  and CCN concentrations reaching  $1000 \text{ cm}^{-3}$  over the southern Central Valley, including the location of Area 5 in Figure 12.

The pristine clouds with large drops and warm rain processes produced a continuum of drop sizes from the cloud drops through the drizzle sizes to the small rain drops. In contrast, clouds that grew to heights with cold temperatures but had suppressed coalescence due to large CCN concentrations still produced mixed-phase precipitation, mainly in the form of graupel. Such clouds produced distinctly different size distribution of the hydrometeors, which was separated from the cloud drop DSD. That is, there were no intermediate-sized drops. Model simulation studies showed that the decreased cloud drop sizes also reduce the mixed-phase precipitation, but the extent of this possible effect from the cloud physics measurements remains to be documented.

Similar response of clouds and precipitation-forming processes to aerosols is apparent also in all the other research flights of SUPRECIP-2, as shown in the next subsection. The continued analyses and evaluation of the aircraft measurements provides compelling evidence for the detrimental role of anthropogenic aerosols on orographic precipitation in California, and they explain how a climatological trend of increased CCN aerosols would cause the climatologically observed trends of reduced orographic precipitation in the southern and central Sierra Nevada. Plots of flight tracks and plotted data for flights of the cloud physics and aerosol aircraft on the other days of SUPRECIP-2 are provided in Appendix E.

### **3.1.2. Ensemble Results**

The research team analyzed all of the cloud passes on all the SUPRECIP-2 flights to determine the cloud depth necessary for each cloud to develop precipitation size particles as a function of the measured sub-cloud CCN concentrations. This analysis was conducted by determining the DL for each measurement, where the modal liquid water drop diameter is defined as the drop diameter having the greatest LWC. The dependence of DL on the CCN for all the measured clouds is provided in Figure 13. This parameter has been used elsewhere, as shown in Figure 14, which provides the drop size for the modal LWC as a function of height for several regions and weather regimes around the world. The precipitation threshold was found to be  $D(\text{LWC}) = 24 \text{ }\mu\text{m}$  (Andreae et al. 2004), or DL24. From Figure 14 one can determine the typical cloud depths necessary for clouds to reach this precipitation threshold.

The results of the analysis of the SUPRECIP-2 cloud passes are presented in Figure 13. Each dot on the figure represents the DL and its height above cloud base (H) for one cloud penetration. A cloud



penetration was defined as a sequence of at least three seconds of CDP droplet concentration larger than  $20 \text{ cm}^{-3}$  and CDP LWC larger than  $0.001 \text{ grams per cubic meter (g/m}^3\text{)}$ . For each such penetration the average number of droplets in every size bin was calculated, and this calculation gave the average size distribution for that penetration. Plotting the LWC density (for each bin normalized to the bin width) made it possible to derive the DL for each penetration manually. Only convective or cloud elements (mostly embedded) entered this analysis. Embedded small convective elements constituted much of the orographic clouds that formed at the foothills of the Sierra Nevada. Layer cap clouds dominated near the crest, but even they were mostly composed of embedded convection with elevated bases. Due to the uncertainty of cloud base height of these clouds, the clouds that were included in Figure 13 were formed mostly at the foothills and lower to mid-level western slopes of the Sierra Nevada.

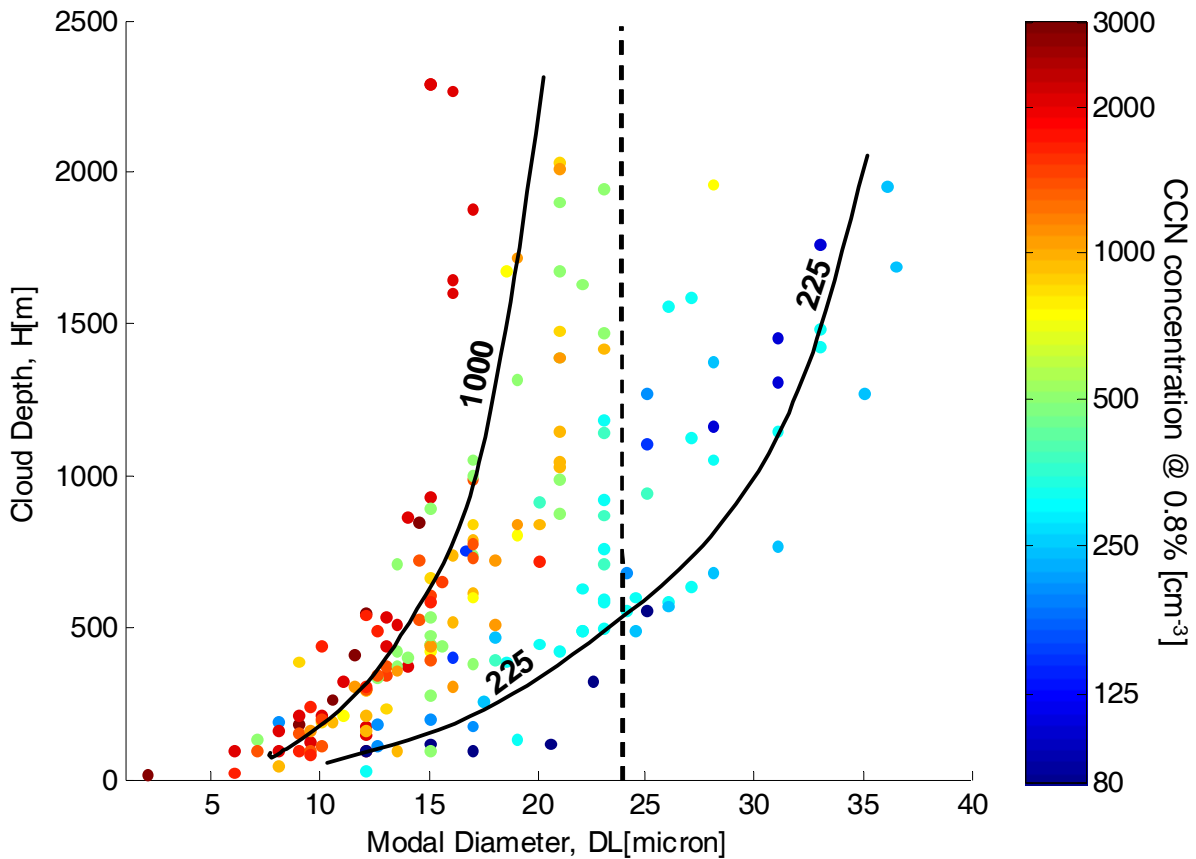


**Figure 13. Scatter plot of the modal liquid water drop diameter (DL) vs. the distance above cloud-base height. Each plotted point has been colorized according to the scale on the right where browns, reds, and yellows indicate cloud passes with high sub-cloud CCN concentrations and blue points indicate cloud passes having low sub-cloud CCN concentrations. The vertical line marks the threshold for formation of precipitation-sized drops, when  $DL = 24 \mu\text{m}$ . The two lines are the approximated contours of 225 and 1000  $\text{CCN cm}^{-3}$ , as done by the contouring routine of MATLAB. The contouring was done after transferring the individual data points to a surface by linear interpolation and initial smoothing.**

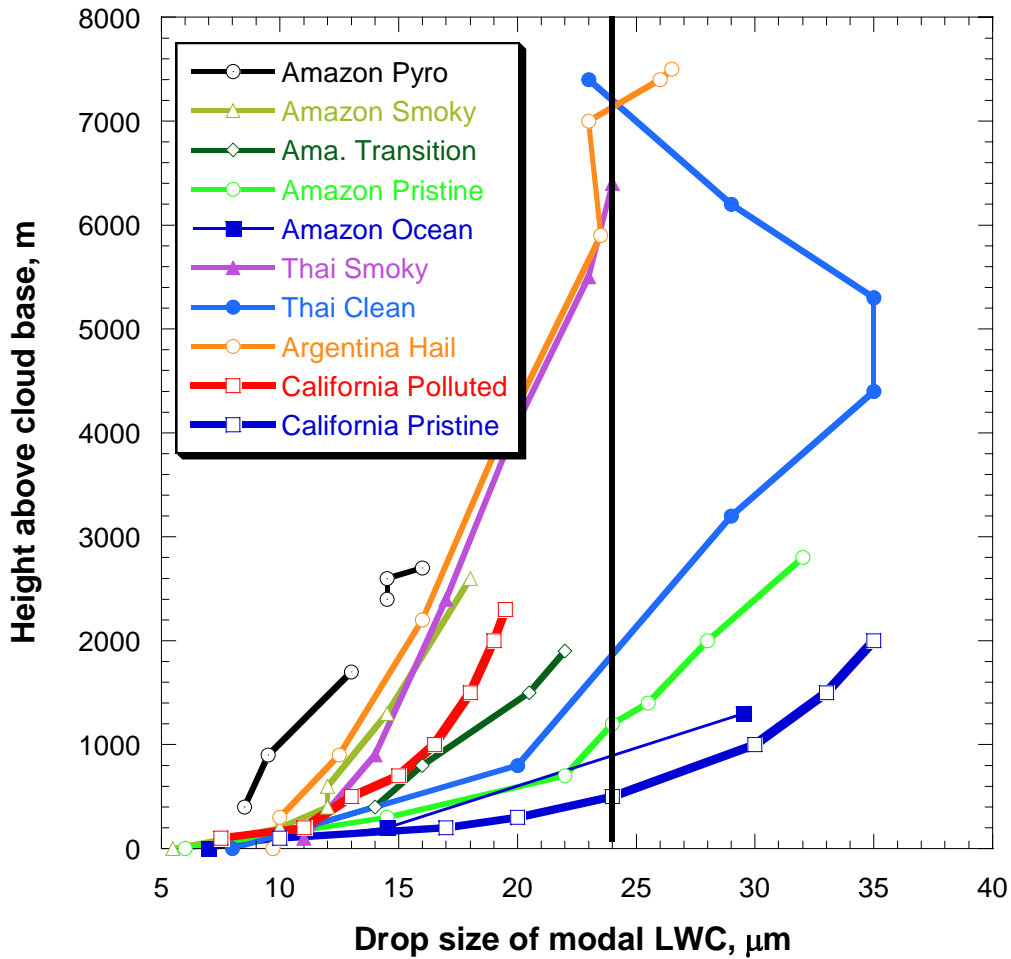


Figure 14. The global context of the dependence of the drop size modal LWC DL on height above cloud base and temperature. The lines, according to their order in the legend, are: Amazon pyro-Cb, smoky, transition, pristine over land and pristine over ocean clouds (Andreae et al. 2004); Thailand pre-monsoon smoky and monsoon relatively clean clouds (Andreae et al. 2004); Argentina microphysically continental hail storms (Rosenfeld et al. 2006); California polluted and pristine clouds (Figure 13 of this study). The vertical line at DL=24 μm represents the warm rain threshold.

To be able to compare penetrations from different clouds and from different days, the cloud base height was subtracted from the penetration altitude, to get the distance of the penetration from the cloud's base. The determination of the cloud's base is not always simple and straightforward because cloud

base height can vary significantly even during a flight. Therefore, in some cases the cloud base height needed to be adjusted so that the DL versus Cloud Depth (on a logarithmic scale) would fall approximately on a straight line (because the droplets grow very fast near cloud base and then at a decreasing rate thereafter (only when coalescence is not playing an important role). This uncertainty in the exact cloud base height leads to some uncertainty in the lowest parts of Figure 13.

Lastly, the color of each small circle is determined by the aerosol-aircraft-measured CCN concentration in the vicinity and below the bases of the penetrated clouds at the maximum supersaturation of  $\sim 0.85\%$ . The scale of the coloring is logarithmic, to increase the definition/resolution at low CCN concentrations.

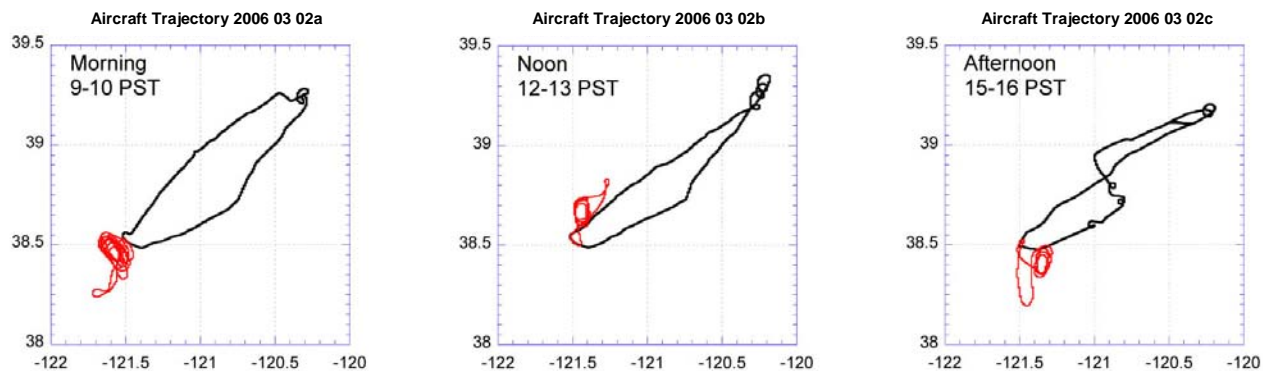
Figure 13 shows that the difference in DL between clouds developing in polluted air (high CCN concentrations) and clouds developing in clean air becomes more and more pronounced with height. The DL of polluted clouds having high CCN concentrations is significantly smaller higher in the clouds, because it increases more slowly with cloud depth than in clouds with low CCN concentrations. The clouds need to be deep enough and the DL needs to reach  $\sim 24 \mu\text{m}$  before significant warm rain can occur. Therefore, the differences in the (warm) precipitation processes become larger higher in the clouds, at least up to 2–2.5 km above their bases, which was reached by the cloud physics aircraft. Because deeper clouds have a greater potential to precipitate large amounts of water, Figure 13 indicates that the aerosols influence the precipitation amounts from these clouds. This serves as evidence of the direct connection between pollution aerosols and precipitation suppression.

Figure 14 shows the global context of the height-DL relations found for pristine and polluted clouds in the study area. According to Figure 14, the pristine clouds in California precipitated at heights starting at 0.5 km, shallower than in the pristine tropical clouds. The polluted clouds in California had larger drops than the respective smoky clouds in the Amazon and Thailand, reflecting the much greater concentration of smoke CCN there than exist currently in the California air pollution during rainy days. This means that the precipitation in these California clouds could be suppressed further if the air pollution concentrations become even greater.

### **3.2. Diurnal Aerosol Variability**

All of the analyses to this point indicate that the ingested aerosols determine cloud internal structure, either promoting or suppressing precipitation formation. There are very strong indications that anthropogenic aerosols generated within California act to decrease the droplet sizes and suppress coalescence processes and precipitation, especially in Sierra orographic clouds. To understand these processes it is important to document the evolution of these aerosols and their effects on clouds during the diurnal cycle. There was an opportunity to do this on March 2, 2006 when each of the research aircraft conducted three flights. Figure 15 shows their flight tracks. Note that the aerosol aircraft stayed close to Sacramento on all three flights because of the showery weather, flying according to visual flight rules in ascending and descending orbits from roughly 1000 to 10,000 ft. The cloud physics aircraft had no such VFR restrictions and flew the tracks as shown.





**Figure 15. The flight tracks for the aerosol (red) and cloud physics (black) aircraft for the three flights on March 2, 2006**

Figure 16 shows plots as a function of height of the CN (total aerosols) and CCN (raw and adjusted to 0.9% supersaturation) concentrations in  $\text{cm}^{-3}$  measured by the aerosol aircraft on the three flights of March 2, 2006 (top three panels) and the corresponding plots as a function of height of the droplet concentrations and sizes ( $r_e$ ) measured by the cloud physics aircraft on its three flights of the day (lower three panels).

Beginning with the top three aerosol plots, it is evident that the aerosol concentrations are highest at the low altitudes in the morning. By the late morning and afternoon, however, the aerosol concentrations have decreased substantially at low altitudes while increasing above as convective currents carry the aerosols to higher altitudes. Thus, the aerosols at an elevated elevation should show a strong diurnal cycle. Indeed this was the case on this day as shown in Figure 17 for the Blodgett Forest Research Station (at an elevation of 1314 m) where aerosol measurements were made throughout SUPRECIP-2 by Desert Research Institute (DRI) CCN spectrometers (Hudson 1989) and a TSI 3010 CN counter. In referring to the Blodgett aerosol plots in Figure 17 note that there is a gap in the midday data due to a power failure. Even so, a strong diurnal cycle is evident in the plots. The vertical blue lines in the figure indicate the earliest (0901 PST) start and latest (1621 PST) end times for the flights of the day. Fortunately, some aerosol data were collected during the flight period despite the substantial data gap. At noon local time (1200 PST) the CCN at 1% SS and CN concentrations measured by the aerosol aircraft at the altitude of the Blodgett station but more than 100 km distant to the southwest were roughly 220 and 1700 particles  $\text{cm}^{-3}$ , respectively. At Blodgett itself the CCN and CN measurements at noon just before the data stream ended were 600 and 1200 particles  $\text{cm}^{-3}$ , respectively. This is reasonable agreement when one considers the physical distance between the Blodgett site and the orbiting aircraft at this time on March 2, 2006.

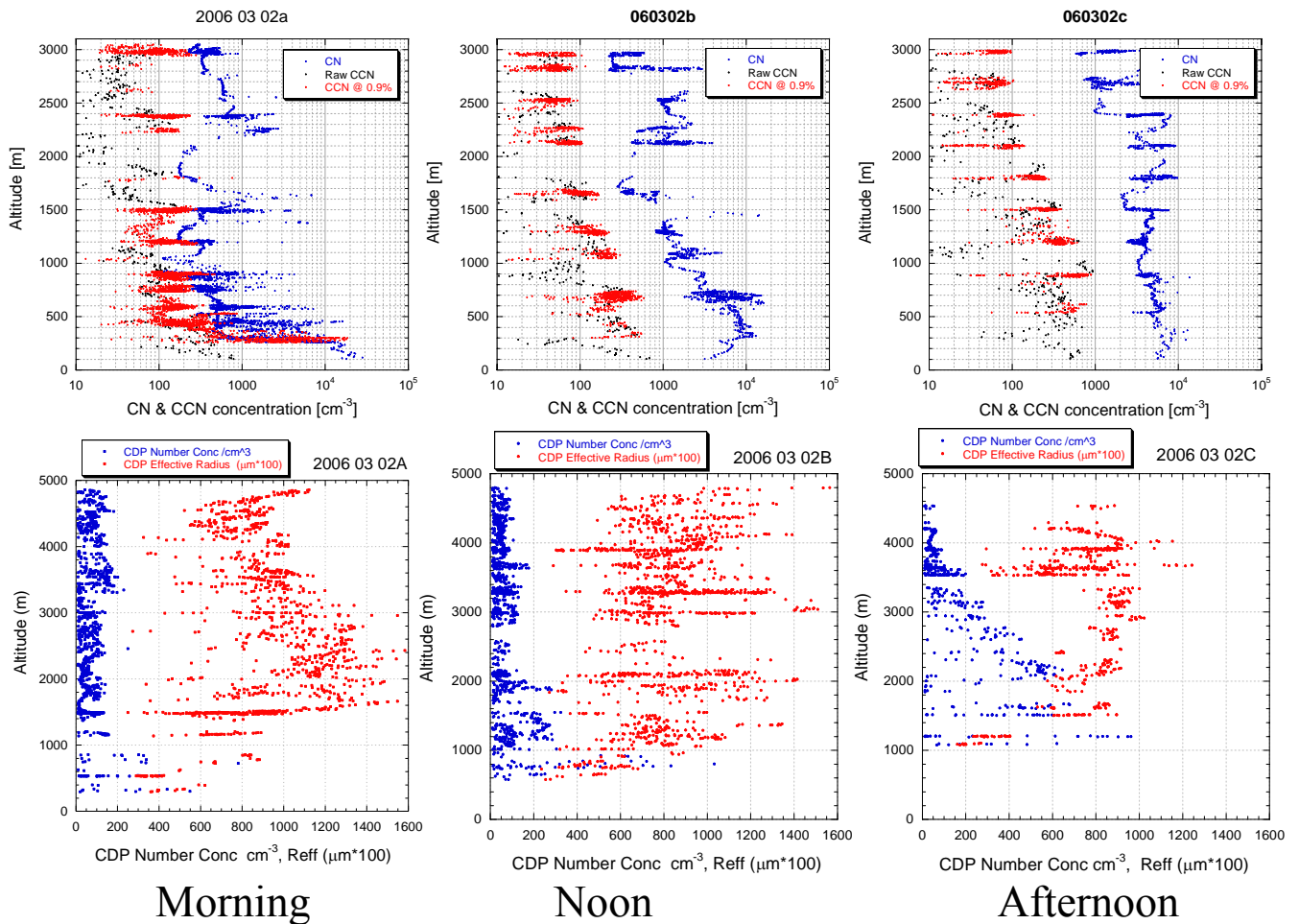


Figure 16. Plots as a function of height (in m) of the CN (total) and CCN concentrations ( $\text{cm}^{-3}$ ) measured by the aerosol aircraft on the three March 2, 2006, flights during its step-climb to 3 km altitude (top three panels) and the corresponding plots as a function of height (in m) of the droplet concentrations and sizes (effective radius) measured by the cloud physics aircraft on its three flights of the day (lower three panels). The red dots in the upper panels show the adjusted CCN measurements (to 0.9% supersaturation) only during horizontal flight (ascent rate  $< \pm 3$  m/s). This adjustment was done to take into account the varying super-saturations (in the range of  $\sim 0.1\%$ – $0.85\%$ ) and because decreases in the raw CCN concentrations were noted while the aircraft was ascending. The black dots are the raw CCN measurements.

### March 2, 2006, Blodgett, CA

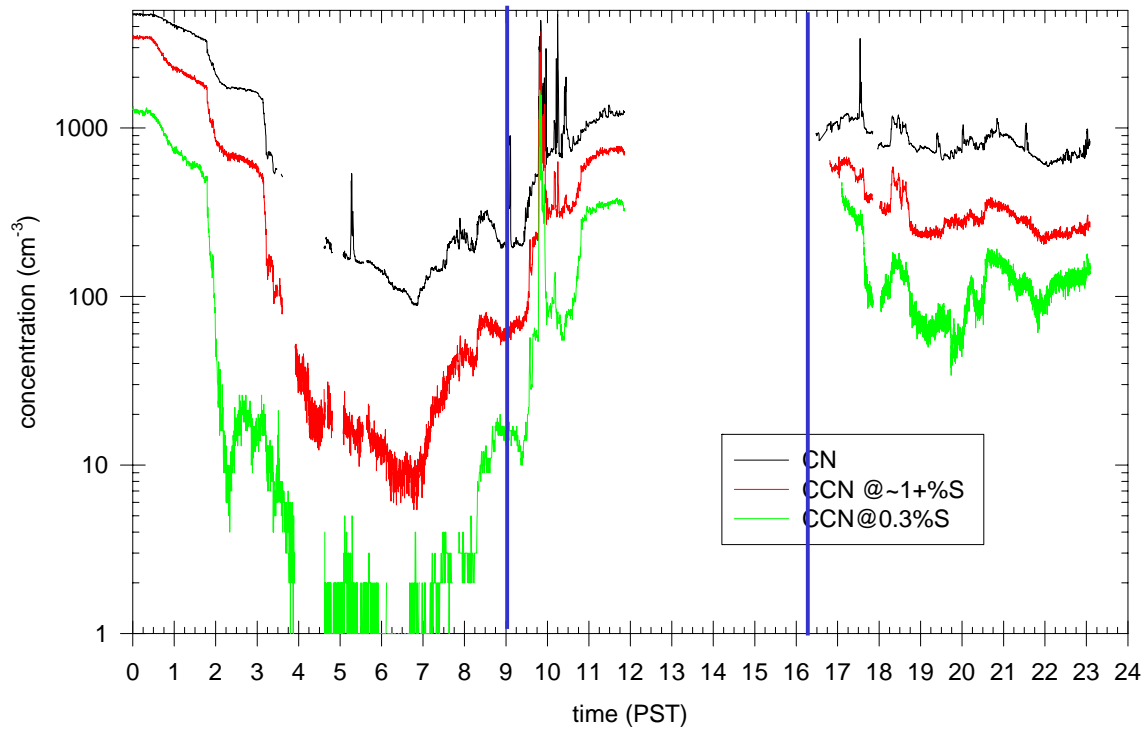
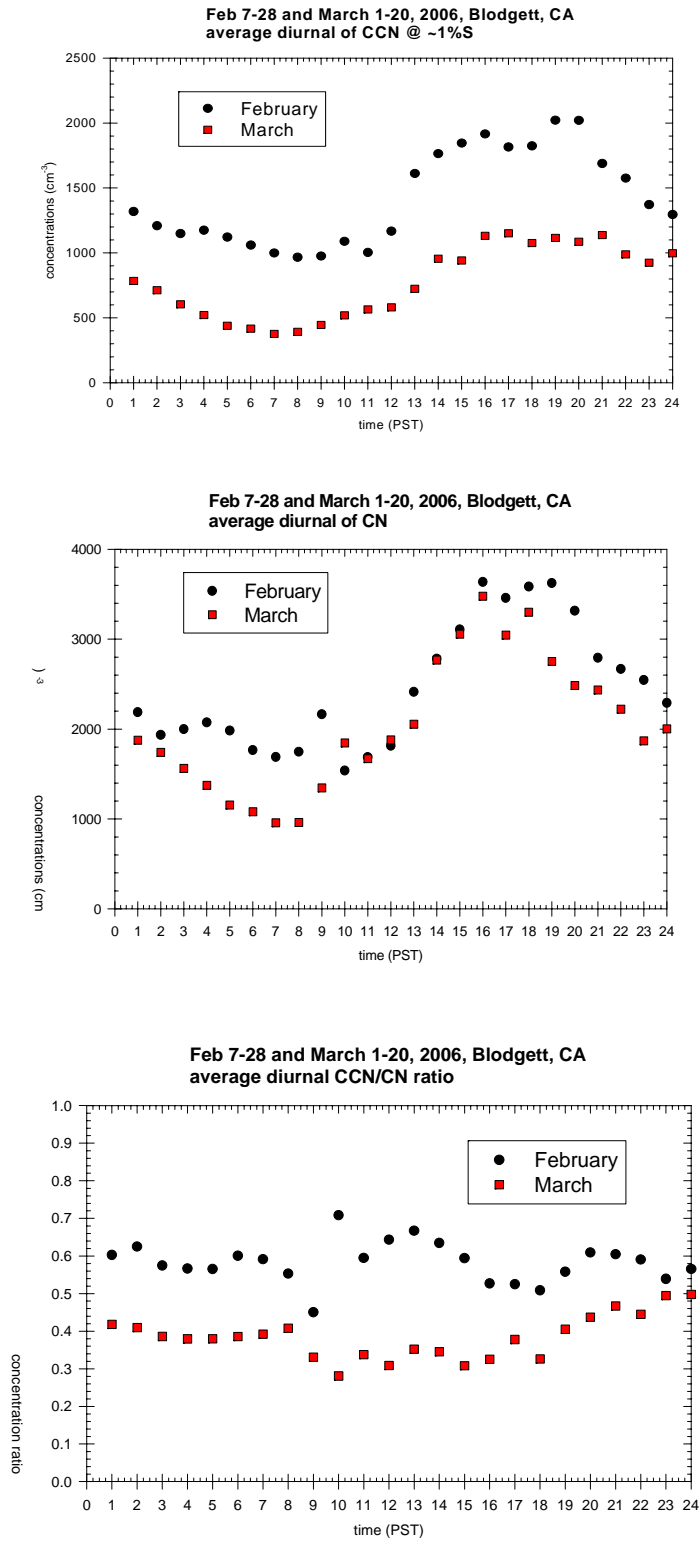


Figure 17. Plots of the CCN (at two supersaturations) and CN aerosols observed at the Blodgett Forest Research Station (1314 m elevation) on March 2, 2006. Despite a gap in the data stream, a strong diurnal cycle is evident in the plots. The vertical blue lines enclose the period (0901 to 1621 PST) when the research aircraft were flying on this day.

Source: Desert Research Institute.

Referring back to Figure 16 for the plots of cloud droplet concentrations and  $r_e$  from the cloud physics aircraft observations (bottom three panels), it can be seen that the changes in the droplet measurements were associated with the changes in the aerosols. With respect to the morning flight, the droplet concentrations were highest (up to  $800 \text{ cm}^{-3}$ ) and their sizes were smallest ( $< 9 \text{ }\mu\text{m}$ ) near the cloud base of 500 m. (To obtain the effective radii sizes, divide the abscissa scale by 100.) Above 1000 m, however, the drop concentrations were  $< 200 \text{ cm}^{-3}$  and the  $r_e$  were as high as  $16 \text{ }\mu\text{m}$ . By the midday flight the cloud bases had risen to 800 m, where the CCN aerosol concentrations reached as high as  $1000 \text{ cm}^{-3}$ . The changes were greatest for the afternoon flight (lower right panel). By this time cloud base was just above 1000 m, the CCN concentrations had increased to  $500 \text{ cm}^{-3}$  over a considerable depth (about 2000 m) above cloud base, and the droplet sizes were much smaller (mostly  $< 10 \text{ }\mu\text{m}$  diameter) between cloud base and 5000 m altitude. The changes were quite appreciable relative to what was measured during the morning flight. The low-level aerosols had clearly been transported upward, increasing the droplet concentrations with height and decreasing their sizes in clouds that had ingested them.

The diurnal changes in aerosol concentrations that were documented by aircraft on March 2, 2006 are typical for the region, as is shown in the February and March 2006 mean CN and CCN aerosol plots versus time at the Blodgett Research Station (Figure 18). Note that the amplitude of the aerosol oscillation at Blodgett is about a factor of two for the CN and CCN aerosols, with the minimum and maximum concentrations in both months occurring at 0700 PST and 1900 PST, respectively. The counts were higher in February than in March 2006 because it was the drier and “dirtier” of the two months.



**Figure 18. Mean time (Pacific Standard Time) plots for February (black) and for March (red) 2006 of the CCN (top) and CN total aerosol (middle) concentrations measured at the Blodgett Research Station by Dr. Jim Hudson of the Desert Research Institute. Plots of the ratio CCN/CN in February (black) and March (red) are given in the bottom panel. The CCN aerosol measurements were made at a supersaturation of 1%.**

The plots of the aerosols on March 2, 2006, show that they originate at the Earth's surface and that they are transported upward by convective currents during the day. This is why the maximum aerosol concentrations are not reached at Blodgett until late in the afternoon. It also means that the greatest suppressive effect of aerosols on clouds will take place late in the day and the subsequent evening when the cumulative heating will produce the convective currents necessary to carry the pollution aerosols into the clouds. Assuming that the physics is correct, the maximum suppressive effect of aerosols should be most noticeable in spring storms when the sun is stronger, the heating is greater, the resulting convective currents are stronger, and the photochemical processes leading to the formation of aerosols are most active.

This hypothesis was tested by examining the precipitation records at two paired (mountain and valley) sites. The first was at Cuyamaca (a mountain station to the east northeast of San Diego) versus the precipitation record at San Diego itself. These paired stations were chosen because of their long, high-quality precipitation records that extend back to 1885. These stations also figured prominently in the paper by Givati and Rosenfeld (2004) in which they laid out their analysis methods. In the Cuyamaca/San Diego case, the analysis of the orographic enhancement factor was conducted separately for the fall (November through January) and spring (February through April) months in each year. The usual scatter plot with best fit lines of the orographic precipitation enhancement ( $R_o$ ) factor for fall and spring is provided in the left panel of Figure 19, where  $R_o$  is defined as the ratio of the precipitation at a mountain station (Cuyamaca) to the precipitation at the upwind lowland plains or coastal station (San Diego). Typically,  $R_o$  is examined over many years. Note that, as predicted, the loss in  $R_o$  over the years in the spring (-29%) is nearly twice the loss in  $R_o$  over the years in the fall (-15%). The second paired stations were gages at Placerville in the Sierra mountains versus Sacramento in the Sacramento Valley. The same pattern is evident with the stronger decrease in  $R_o$  evident in the spring (-27%) than in the fall (-17%). Here again, additional pieces of the puzzle have fallen into place, identifying anthropogenic aerosols for the progressive suppression of orographic precipitation in the California Sierra Nevada.

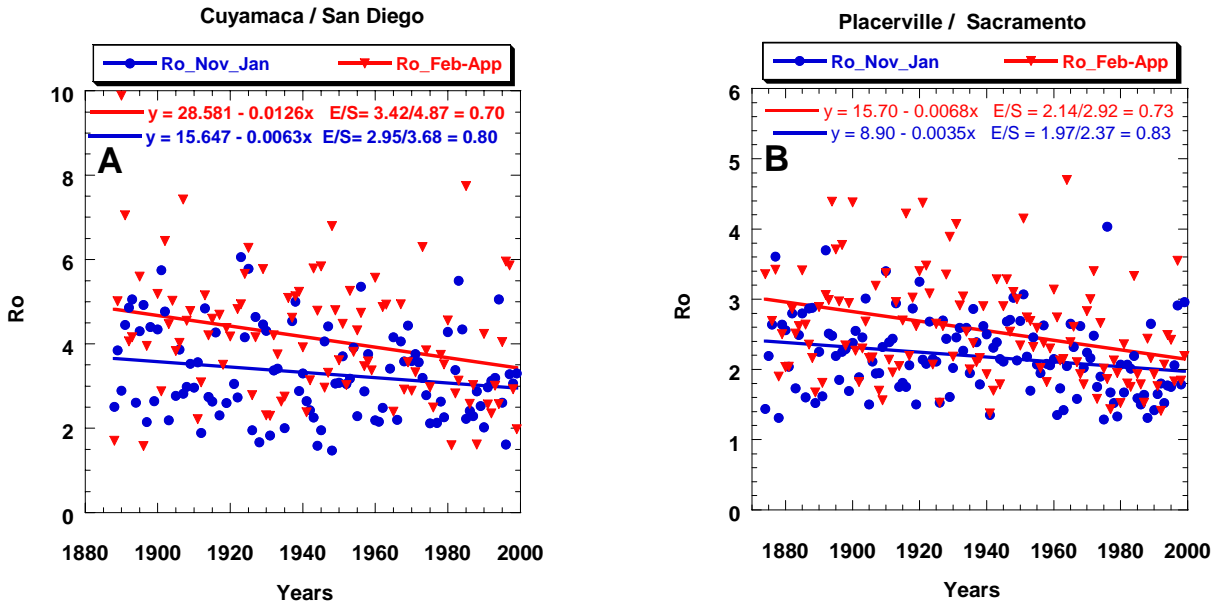


**Figure 19.** Scatter plot of the orographic precipitation enhancement factor (Ro) in the fall (blue points) and spring (red points) for the years 1885 to 2000 for Cuyamaca vs. San Diego (panel A), where Ro is defined as the ratio of the precipitation at the mountain station (Cuyamaca) to the precipitation at the upwind lowland plains or coastal station. Panel B shows the same for Ro between a gauge cluster in Placerville versus a cluster in the Sacramento area. The apparent effect of pollution on precipitation at the mountain station is obtained by taking the ratio of Ro at the end of the period of interest to Ro at the outset of the period, where the ending and starting Ro values are obtained from the best-fit line to the scatter plot. In these instances the analyses were done separately for the fall and spring months. Although precipitation losses occurred in both the fall and spring, the losses were greater in the spring (i.e., -27% to -30%) than in the fall months (i.e., -17% to -20%) because the sun is stronger in the spring months during which convective currents would more readily transport pollution aerosols to higher altitudes.

### 3.3. Spatial Aerosol Distribution

Of great interest in SUPRECIP-2 were the spatial distribution of CN and those aerosols that acted as CCN at supersaturations up to 0.9%. By compositing all of the flights of the aerosol aircraft it was hoped that an informative pattern would emerge as a function of space, time, altitude, and wind regime. The first step of the analysis was a printout of the adjusted CCN observations made by the aerosol aircraft on all flights when it was flying below 5000 ft, as shown in Figure 20. The boundary-layer winds were not considered in making this plot. The observations were color-coded along the track. The portions of the track that are orange to brown had CCN concentrations  $> 1000$  particles/cm<sup>3</sup> while those portions that have light blue to dark blue coloration had CCN concentrations  $< 100$  particles/cm<sup>3</sup>. The pattern proved to be somewhat of a surprise because the highest CCN concentrations were found in the Central Valley, mostly to the east and south of Sacramento and not so much in the coastal urban areas as had been expected. Although high counts had been experienced intermittently in the San Francisco/Oakland areas, the high counts farther east cannot be explained by the simple transport of pollutants from the west. This suggests significant generation of pollutants in the Central Valley itself. These findings are consistent with those published by Chow et al. (2006) resulting from the analysis of an extensive surface-measurement program for the measurement of aerosol concentrations and their chemistry in this region.



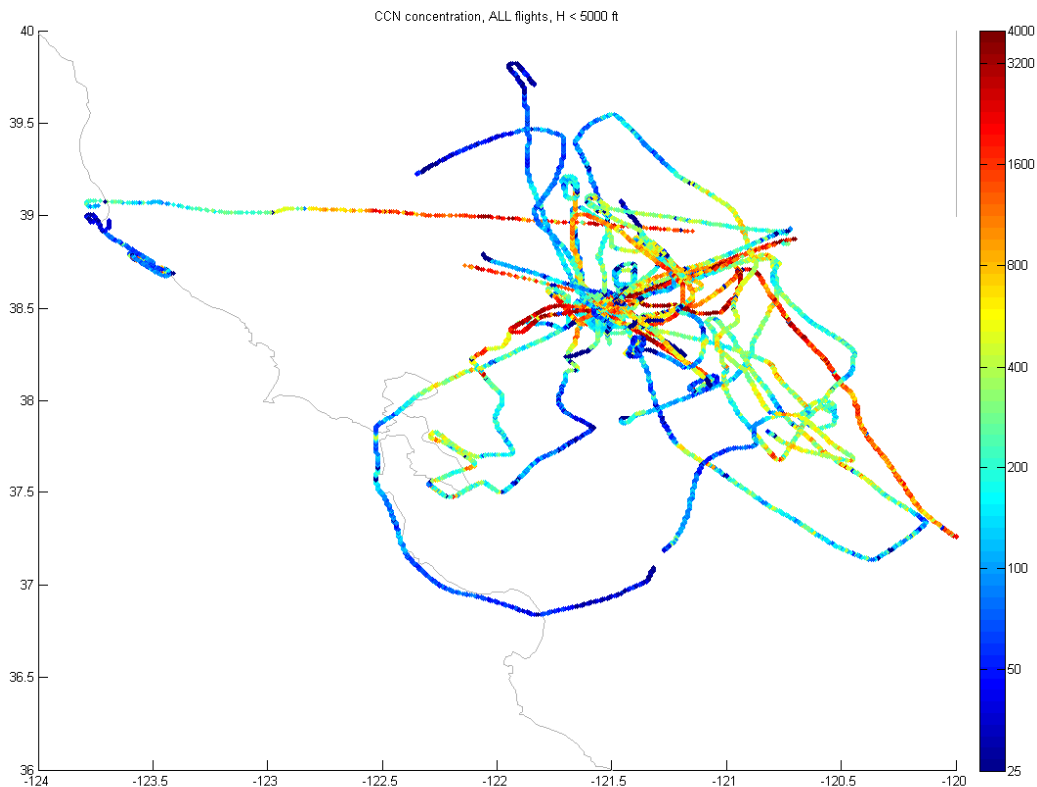


**Figure 20. A colorized plot summary of the CCN measurements made on all flight days without wind partitioning during SUPRECIP-2 when the aerosol aircraft was flying below 5000 ft, almost exclusively below cloud base. The X and Y axes are deg. longitude and deg. latitude, respectively. According to the legend, the portions of the track when the CCN readings exceeded  $1000/\text{cm}^3$  are orange changing to dark brown at readings of  $4000/\text{cm}^3$ . The portions of the track when the CCN readings were  $< 100/\text{cm}^3$  begin at light blue and change to dark blue for the lowest CCN concentrations. Note that the highest CCN readings were in the Sacramento area and southeastward to the Sierra foothills.**

The next step was the compositing of the flights that had similar boundary-layer winds, because the movement of the aerosols obviously depends on the low-level altitude ( $< 5000$  ft) winds. Streamline maps for the surface winds were obtained from the National Oceanic and Atmospheric Administration's (NOAA's) Air Resources Laboratory for each flight day. Figure 21 provides an example of the streamline map for the afternoon flight on February 28, 2006 (already 00Z on March 1, 2007), the flight discussed earlier.

The CCN plots partitioned by wind direction were not any more informative than the overall plot in Figure 20, because there was not that much variability in wind direction on the flight days. The plot for southwesterly winds is given in Figure 22 for flights at  $< 5000$  ft. The plot is similar to that in Figure 20 without wind partitioning. The rest of the wind-partitioned plots were not any more informative because of the rather small sample.

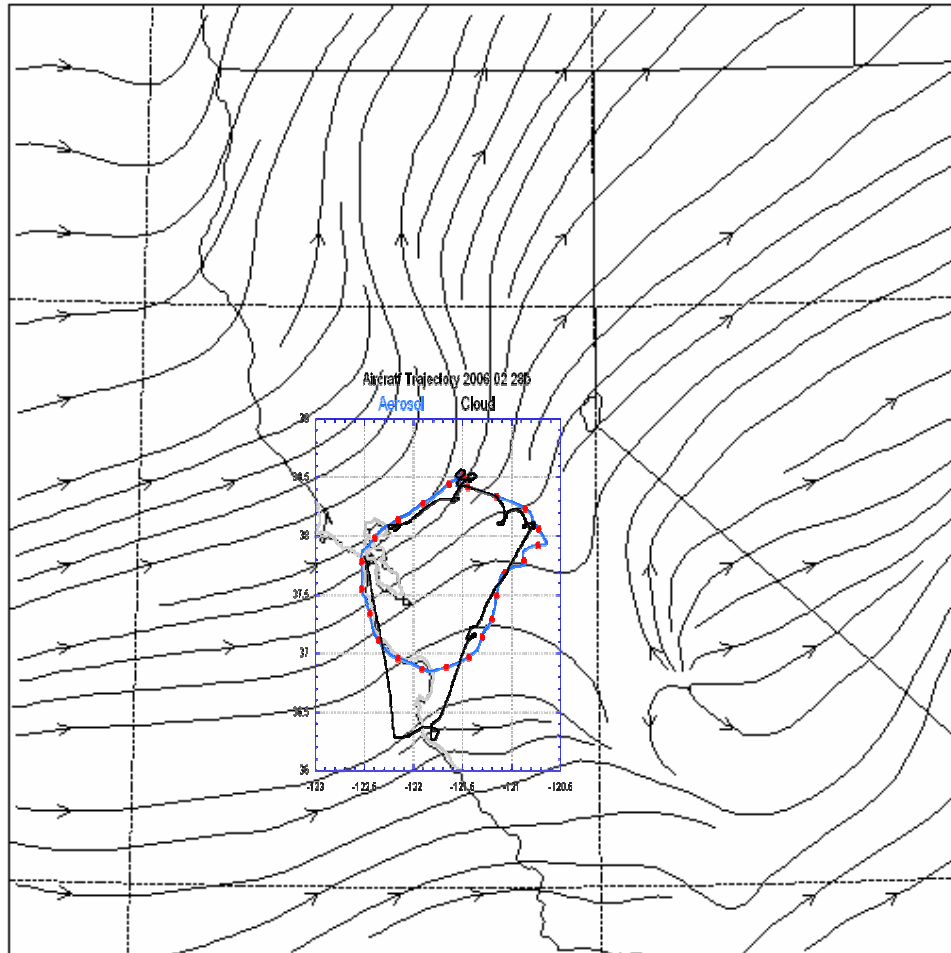


NOAA Air Resources Laboratory

This product was produced by an Internet user on the NOAA Air Resources Laboratory's web site. See the disclaimer for further information (<http://www.arl.noaa.gov/ready/disclaim.html>).

EDAS40 Archive

METEOROLOGICAL DATASET INFORMATION  
Initialization time: 00 UTC 01 MAR 2006

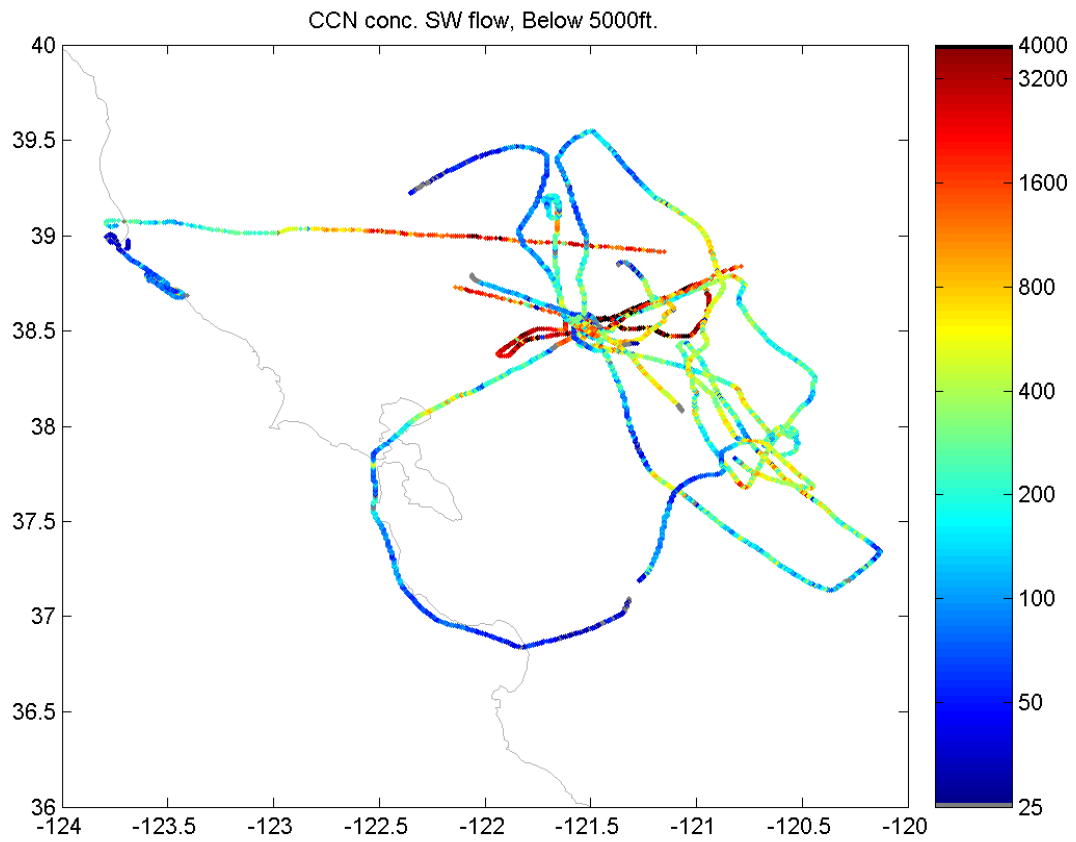


NATIONAL OCEANIC AND ATMOSPHERIC ADMINISTRATION - AIR RESOURCES LABORATORY

STREAMLINES

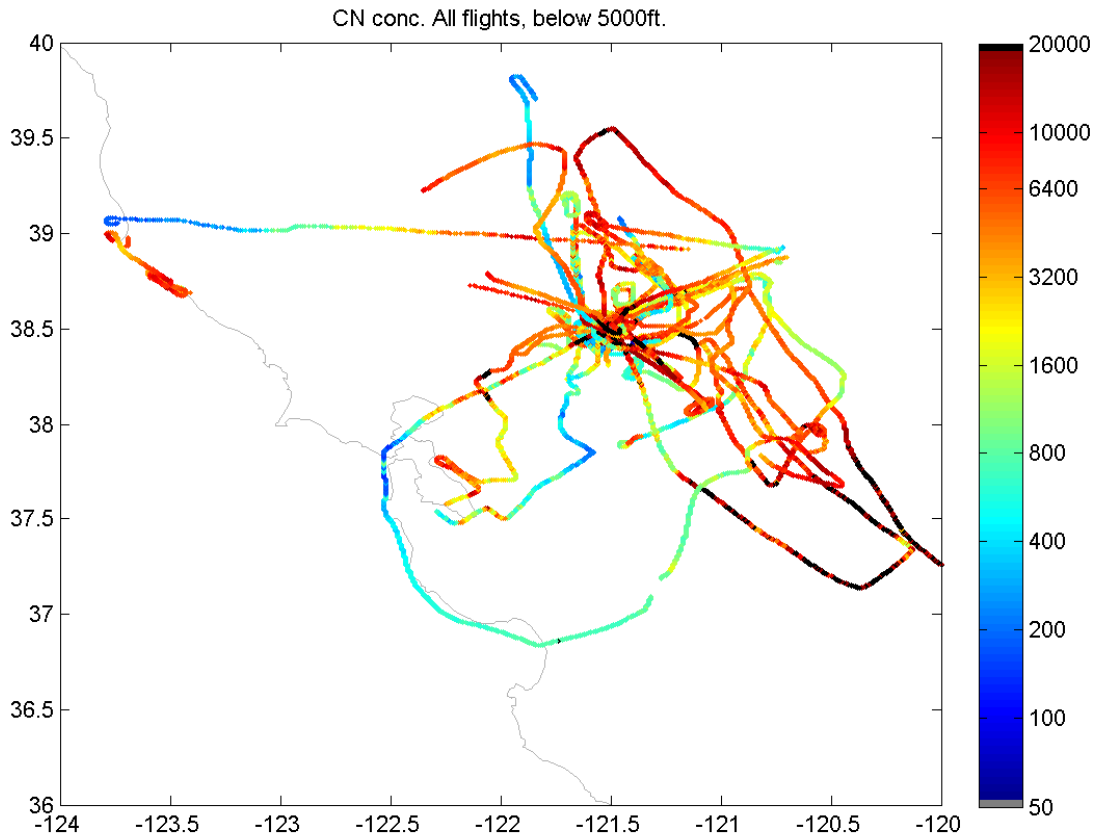
STRM (KNTS), LVL= SFC , 00 UTC 01 MAR 2006 (+ 00 H )

Figure 21. Surface streamline map for Central and Northern California at 00 UTC on March 1, 2006, produced by NOAA's Air Resources Laboratory. The flight tracks of the cloud physics (black) and aerosol aircraft (blue with red dots every 5 minutes along the track) have been superimposed on the streamline presentation. The flight tracks are the same as those presented in Figure 6.



**Figure 22. The same as for Figure 20 but for southwesterly surface wind flows. Units for the X and Y axes are degrees west longitude and degrees north latitude, respectively.**

The total aerosol plots of condensation nuclei are also of considerable interest. The overall plots for all flights without wind partitioning are given in Figure 23. Not surprisingly, it bears a strong resemblance to the overall CCN plots, except in this case the counts are much higher, especially in the central and eastern portions of the Central Valley, as is the case with the overall CCN plots. With such a heavy aerosol loading it comes as no surprise that this is the area in the Sierra where the suppression of precipitation and runoff is greatest.



**Figure 23. The same as in Figure 20 but for the CN (total aerosol) measurements**

It is informative to look at plots of the ratio of CCN to CN to determine what fraction of the total aerosol serves as CCN. This is done in Figure 24 for all flights when the aerosol aircraft was flying at an altitude < 5000 ft. Although there are exceptions, the CCN/CN ratio ranges from 0.1 to 0.2 over most of the map. This is considerably smaller than the mean ratio documented at the Blodgett aerosol site at which the mean ratio CCN/CN was about 0.6 in February and 0.4 in March (see Figure 18). The reason(s) for the differing mean ratios is unknown. It may be due to CN concentrations closer to their sources, because the CN tend to decrease farther from their immediate sources.

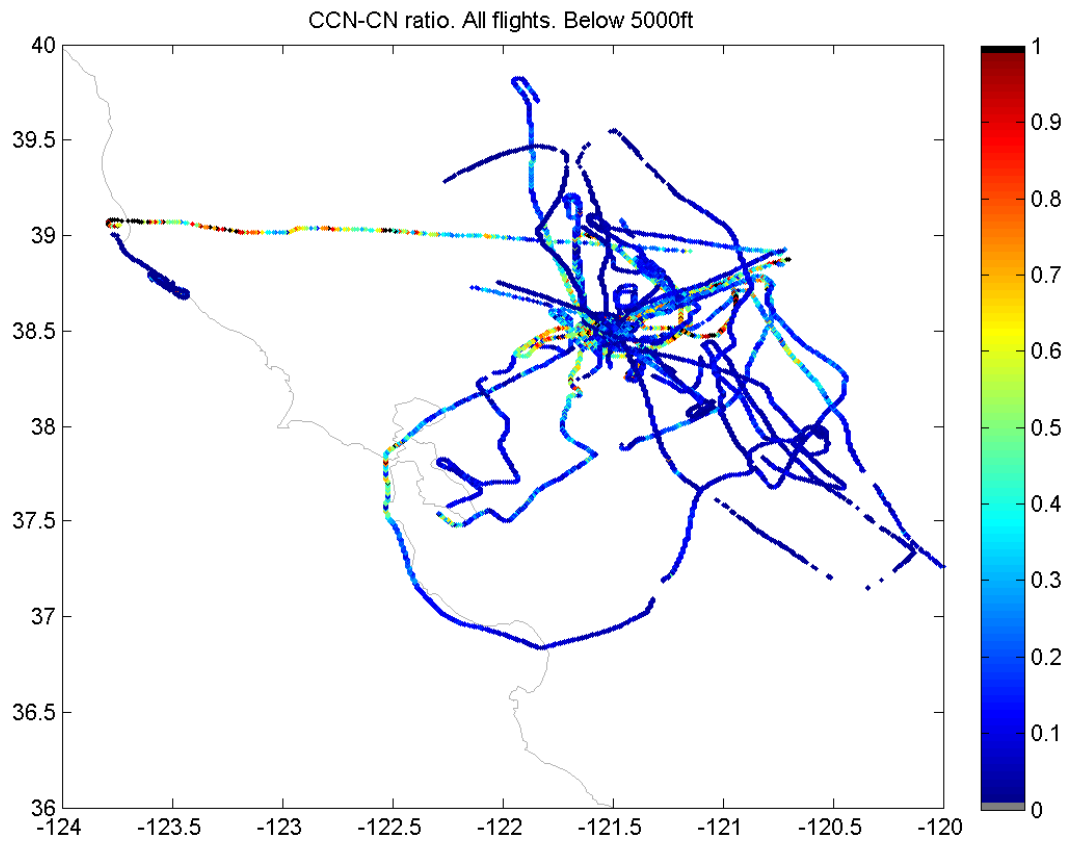


**Figure 24.** The same as for Figure 20 but for the ratio of CCN to CN. The colored portion of the track can be related to CCN/CN from the figure legend.



## 4.0 Discussion

The pieces of the research puzzle are slowly falling into place with respect to the trend of decreasing orographic precipitation over many areas of the globe and attendant losses in runoff (Woodley Weather Consultants 2007) and flows from underground springs (Rosenfeld et al. 2007). With respect to California it was determined also that the Pacific decadal oscillation (PDO) and the Southern Oscillation index (SOI) (Allan et al. 1991; Dettinger et al. 2004), cannot explain the observed declining trends in the orographic precipitation enhancement factor ( $R_o$ ) (Rosenfeld and Givati 2006).

These apparent losses in orographic precipitation are not limited to California. Rosenfeld and Givati (2006) expanded the study to the whole western United States, where they showed that  $R_o$  remained stable over hills in the more pristine areas in northern California and Oregon but decreased again to the east of the densely populated and industrialized Seattle area. Similar effects were observed not only in the Pacific coastal areas, but also well inland. Precipitation was decreased by 18% over the mountains to the east of Salt Lake City, Utah, but remained unchanged at the southern extension of the same mountain range (Rosenfeld and Givati 2006; Griffith et al. 2005). Similar effects were found during easterly winds over the eastern slope of the Rocky Mountains downwind (i.e., to the west) of Denver and Colorado Springs (Jirak and Cotton 2006).

The common denominator for the regions suffering losses in orographic precipitation has been found in the multi-spectral satellite imagery that shows decreased cloud-particle ( $r_e$ ) for the affected regions. In California this was addressed using multi-spectral satellite images from polar-orbiting satellites (Woodley Weather Consultants 2007). On each day with a satellite overpass, the multi-spectral imagery was processed to infer the  $r_e$  of cloud particles for the clouds within selected areas within the field of view. This was done because previous studies had shown that areas with small  $r_e$  are slow to develop precipitation. After the satellite inferences had been made they were composited geographically. It was found that  $r_e$  increases more slowly with decreasing temperature in the central and southern Sierra compared to the northern Sierra. The slower increase of  $r_e$  with elevation is the most robust indicator for the slower development with height of precipitation in the clouds. This finding is consistent with the gauge and stream-flow analyses that show that the greatest losses of water occur in the central and southern Sierra (Woodley Weather Consultants 2007). This suggested a major role of CCN pollutants that are ingested by the orographic clouds with consequent suppression of coalescence along the lines of the hypothesis put forth at the outset of this study.

SUPRECIP was designed to address the potential linkages between pollution aerosols and the loss of orographic precipitation and subsequent runoff. SUPRECIP-1 showed a strong positive correlation between the satellite-inferred cloud microphysics and the aircraft-measured cloud microphysics. Thus, it also confirmed that the areas in the central and southern Sierra that were shown by satellite to have smaller  $r_e$  than those in the northern Sierra likely do have suppressed precipitation-forming processes.

Some of this work's reviewers initially were unwilling to concede the probable role of pollution aerosols in bringing about suppressed precipitation, despite indications (see Figures 2, 3, and 4 herein) that this is indeed the case. SUPRECIP-2 made the direct connection between the pollution aerosols and suppressed precipitation-forming processes. The scatter plot of the modal liquid water drop diameter versus the depth above cloud-base height (Figure 13) as a function of the ingested CCN

shows that clouds growing in a polluted environment must reach greater depths to develop precipitation than clouds growing in a more pristine environment where the CCN concentrations are lower.

In looking at the temporal and spatial patterning of the pollution aerosols in California, it was determined that they typically exhibit a strong diurnal oscillation with the strongest upward transport during the late afternoon. Thus, the sampled clouds are more continental in character, with smaller droplet sizes and diminished coalescence at this time of day. The aerosol concentrations were minimal over the ocean and increased after traversing the shoreline, where urban and industrial development has taken place. The aerosols found over the Central Valley were not simply transported from the coastal areas, because on most days the CN and CCN concentrations in the Valley to the Sierra foothills exceeded what was found in the coastal urbanized areas. This is true especially in the central and southern Valley well to the east of sparsely populated coastal regions.

It appears, therefore, that the large aerosol concentrations that are likely suppressing the Sierra orographic precipitation are generated locally in the Valley itself, having unknown specific origins and chemistry. This is consistent with the findings of Chow et al. (2006) from an extensive aerosol measurement program in the San Joaquin Valley. Although transport of pollution aerosols from the ocean and from coastal regions may play a role in the suppression of Sierra orographic precipitation, it would appear to be secondary to the role being played by the local generation of aerosols in regions of highest concentrations. Understanding this role would appear to be the next logical step in this research effort.

A major component of this research effort was model simulation of the effects of aerosols (Lynn et al. 2007). The simulation with clean air produced more precipitation on the upwind mountain slope than the simulation with continental aerosols. After three hours of simulation time, the simulation with maritime aerosols produced about 30% more precipitation over the length of the mountain slope than the simulation with continental aerosols. Greater differences in precipitation amounts between simulations with clean and dirty air were obtained when ice microphysical processes were included in the model simulations.

Thus, the totality of the evidence from the research effort, involving precipitation and stream flow analyses, quantitative satellite measurements, numerical modeling and extensive aircraft measurements of cloud properties and aerosols, makes a strong case for the loss of precipitation and stream flows in the California Sierra Nevada due to the generation of anthropogenic pollutants and their ingestion into Sierra clouds.



## 5.0 Conclusions

SUPRECIP-2 met its primary objective of documenting the effects of pollution aerosols on clouds and their precipitation over the California Sierra Nevada. The aircraft measurements of cloud properties validated the satellite inferences of cloud microphysics. They also verified those regions over which the processed multi-spectral imagery indicated the clouds had small droplet sizes and suppressed coalescence versus those areas where the satellite inferences indicated the clouds had large droplet sizes and coalescence. Those measurements increase the credibility of satellite inferences of altered cloud properties in the central and southern Sierra.

The key uncertainty at the outset of SUPRECIP was whether the altered cloud properties were due to the ingestion of pollution aerosols. Although SUPRECIP 1 gave the first indications of a link between the pollution aerosols and the suppression of precipitation-forming processes, it took SUPRECIP-2, using two cloud physics aircraft, to demonstrate the direct linkage between these aerosols and the regions in the central and southern Sierra Nevada that have suffered losses of orographic precipitation and stream flows. Analysis of several hundred cloud passes has shown that in regions where high concentrations of CCN were measured by the base aerosol aircraft, the clouds had to grow to greater depths to develop precipitation than clouds growing in regions of low CCN concentrations.

The spatial and temporal documentation of the CCN and CN aerosols was highly informative. Although the initial source of the pollution aerosols was clearly the urbanized coastal regions, the pollution aerosols in the Central Valley to the Sierra foothills cannot be explained by simple advection of the pollutants from the coastal urban areas. There is clearly a major source of pollution aerosols in the Central Valley itself and these CCN and CN aerosols are concentrated primarily over the Central Valley from just to the north of Sacramento southward along the foothills to south of Fresno. This is the same region that has been shown through statistical analysis of precipitation and stream-flow records to suffer the greatest loss of winter orographic precipitation and subsequent stream flows.

The pollution aerosols show a strong diurnal oscillation. In the morning these aerosols are concentrated at low levels, but by late afternoon they have been transported upward due to afternoon heating. Thus, the regional clouds are most affected by the pollutants late in the day. The aircraft measurements indicate that the ratio of CCN to CN aerosols is typically 0.10 to 0.20 whereas the measurements at the ground-based (Blodgett) site indicate that the ratios are higher.

The evidence amassed from SUPRECIP and the ancillary precursor research conducted by the authors indicates that the precipitation and stream flow losses are real and due primarily to the ingestion of pollutants by orographic clouds over the Sierra Nevada. Further, the results of model simulations demonstrating the detrimental effects of pollutants on Sierra orographic precipitation give additional weight to the hypothesis put forth at the outset of this study.

Because the local generation of the pollution aerosols in the Central Valley appears to be a greater problem than the transport of pollution from the urbanized/industrialized coastal regions or inland from the Pacific, the next step in the research progression is to document the sources and chemical constituency of the aerosols in the Central Valley.



## 6.0 References

- Allan, R. J., N. Nicholls, P. D. Jones, and I. J. Butterworth. 1991. "A further extension of the Tahiti-Darwin SOI, early SOI results and Darwin pressure." *J. Climate* 4: 743–749.
- Andreae M. O., D. Rosenfeld, P. Artaxo, A. A. Costa, G. P. Frank, K. M. Longo, and M. A. F. Silva-Dias. 2004. "Smoking rain clouds over the Amazon." *Science* 303: 1337–1342.
- Chow, J. S., L.-W. A. Chen, J. G. Watson, D. H. Lowenthal, K. A. Magliano, K. T. Turkiewicz, and D. E. Lehrman. 2006. "PM<sub>2.5</sub> chemical composition and spatiotemporal variability during the California Regional PM<sub>10</sub>/PM<sub>2.5</sub> Air Quality Study (CRPPAQS)." *J. Geophys. Res.* Vol. 111. D:10.1029/2005 JD006457.
- Dettinger, M., K. Redmond, and D. Cayan. 2004. "Winter Orographic Precipitation Ratios in the Sierra Nevada – Large-Scale Atmospheric Circulations and Hydrologic Consequences." *J. Hydromet.* 5: 1102–1116.
- Gerber, H. 1996. "Microphysics of marine stratocumulus clouds with two drizzle modes." *J. Atmos. Sci.* 53: 1649–1662.
- Givati, A., and D. Rosenfeld. 2004. "Quantifying precipitation suppression due to air pollution." *Journal of Applied Meteorology* 43: 1038–1056.
- Givati, A., and D. Rosenfeld. 2005. "Separation between Cloud Seeding and Air Pollution Effects." *Journal of Applied Meteorology* 44: 1298–1314.
- Givati, A., and D. Rosenfeld. 2007. "Possible impacts of anthropogenic aerosols on water resources of the Jordan River and the Sea of Galilee." *Water Resources Research* Vol. 43, W10419, doi:10.1029/2006WR005771.
- Griffith, D. A., M. E. Solak, and D. P. Yorty. 2005. "Is air pollution impacting winter orographic precipitation in Utah? Weather modification association." *J. Wea. Modif.* 37: 14–20.
- Heymsfield, A. J., and G. M. McFarquhar. 2002. "Microphysics in INDOEX clean and polluted trade cumulus clouds." *Journal of Geophysical Research* 106: 28,653–28,676.
- Hudson, J. G. 1989. "An instantaneous CCN spectrometer." *J. Atmos. & Ocean. Techn.* 6: 1055–1065.
- Hudson, J. G., and S. Mishra. 2007. "Relationships between CCN and cloud microphysics variations in clean maritime air." *Geophys. Res. Lett.* 34, L16804, doi:10.1029/2007GL030044.
- Hudson, J. G., and S.S. Yum. 2001. "Maritime-continental drizzle contrasts in small cumuli." *J. Atmos. Sci.* 58: 915–926.
- Jirak, I. L., and W. R. Cotton. 2006. "Effect of air pollution on precipitation along the Front Range of the Rocky Mountains." *J. Appl. Meteor.* 45: 236–245.
- Lynn B., A. Khain, D. Rosenfeld, W. L. Woodley. 2007. "Effects of aerosols on precipitation from orographic clouds." *J. Geophys. Res.* 112, D10225, doi:10.1029/2006JD007537.

- McFarquhar, G. M., and A. J. Heymsfield. 2001. "Parameterizations of INDOEX microphysical measurements and calculations of cloud susceptibility: Applications for climate studies." *J. Geophys. Res.* 106: 28,675–28,698.
- Rosenfeld, D., and G. Gutman. 1994. "Retrieving microphysical properties near the tops of potential rain clouds by multispectral analysis of AVHRR data." *Atmospheric Research* 34: 259–283.
- Rosenfeld, D., and I. M. Lensky. 1998. "Satellite-based insights into precipitation formation processes in continental and maritime convective clouds." *The Bulletin of American Meteorological Society* 79: 2457–2476.
- Rosenfeld, D. 2000. "Suppression of Rain and Snow by Urban and Industrial Air Pollution." *Science* 287 (5459): 1793–1796.
- Rosenfeld, D., R. Lahav, A. P. Khain, M. Pinsky. 2002. "The role of sea-spray in cleansing air pollution over ocean via cloud processes." *Science* 297: 1667–1670.
- Rosenfeld, D., and W. L. Woodley. 2003. Closing the 50-year circle: From cloud seeding to space and back to climate change through precipitation physics. Chapter 6 of "Cloud Systems, Hurricanes, and the Tropical Rainfall Measuring Mission (TRMM)" edited by Drs. Wei-Kuo Tao and Robert Adler, 234 pp., p. 59–80, Meteorological Monographs 51, AMS.
- Rosenfeld, D., and A. Givati. 2006. "Evidence of orographic precipitation suppression by air pollution induced aerosols in the western U.S." *J. Applied Meteorology and Climatology* 45: 893–911.
- Rosenfeld, D. 2006. Aerosols Suppressing Precipitation in the Sierra Nevada: Results of the 2006 Winter Field Campaign. Presented at the Third Climate Change Research Conference, California Energy Commission, Sacramento, California, 13–15 September 2006. Presentation available at: [www.climatechange.ca.gov/events/2006\\_conference/presentations/2006-09-14/2006-09-14\\_ROSENFELD.PDF](http://www.climatechange.ca.gov/events/2006_conference/presentations/2006-09-14/2006-09-14_ROSENFELD.PDF).
- Rosenfeld, D., J. Dai, X. Yu, Z. Yao, X. Xu, X. Yang, C. Du. 2007. "Inverse relations between amounts of air pollution and orographic precipitation." *Science* 315, 9 March 2007, 1396–1398.
- Woodley Weather Consultants. 2005. *The Use of a Cloud Physics Aircraft for the Mapping of Pollution Aerosols Detrimental to Winter Orographic Precipitation over the California Sierra Nevada*. California Energy Commission, PIER Energy-Related Environmental Research. CEC-500-2005-205.
- Woodley Weather Consultants. 2007. *Physical/Statistical and Modeling Documentation of the Effects of Urban and Industrial Air Pollution in California on Precipitation and Stream Flows*. California Energy Commission, PIER Energy-Related Environmental Research Program. CEC-500-2007-019.
- Yum, S. S., and J. G. Hudson. 2002. "Maritime/continental microphysical contrasts in stratus." *Tellus* 54B: 61–73.

## 7.0 Glossary

CCN	Cloud condensation nuclei
CDP	cloud droplet probe
CIP	cloud imaging probe
cm <sup>3</sup>	cubic centimeters
CN	condensation nuclei (The total aerosol present at the sampled location.)
Deff	effective diameter
DL	modal liquid water cloud drop diameter
DMA	Differential Mobility Analyzer
DRI	Desert Research Institute
DSD	droplet size distribution
dT	temperature difference
H	height above cloud base
IFR	instrument flight rules
IMPROVE	Interagency Monitoring of Protected Visual Environments
km	kilometer
LWC	liquid water content
m	meter
NOAA	National Oceanic and Atmospheric Administration
PIER	Public Interest Energy Research
PM <sub>2.5</sub>	particulate matter equal to or smaller than 2.5 micrometers in size
PST	Pacific Standard Time
pyro-Cb	pyro-cumulonimbus cloud
r <sub>e</sub>	cloud drop effective radii
Ro	The orographic precipitation enhancement factor. Ro is the ratio of precipitation at a hilly or mountain station to the precipitation at a lower plains or valley station.
SS	supersaturation
SOAR	Seeding Operations and Atmospheric Research

<b>SUPRECIP</b>	<b>Suppression of Precipitation</b>
<b>TDMA</b>	<b>Tandem Differential Mobility Analyzer</b>
<b>UC</b>	<b>University of California</b>
<b>μm</b>	<b>micrometer</b>
<b>VFR</b>	<b>visual flight rules</b>

## **Appendices**

Appendices for this report are available in a separate volume: CEC-500-2008-015-AP.

Appendix A. Worldwide Evidence for the Effect of Aerosols on Clouds and Precipitation

Appendix B. Operational Documentation of the SUPRECIP Program

Appendix C. The SOAR Research Aircraft During SUPRECIP-2

Appendix D. The Satellite Methodology Used in the Research Effort

Appendix E. Presentation of Flight Tracks and Plotted Data for Flights of the Cloud Physics and Aerosol Aircraft